

Additive Manufacturing of Self-Sensing Materials

Benyam Alexander Angeria

Civil Engineering, master's level
2022

Luleå University of Technology
Department of Civil, Environmental and Natural Resources Engineering

Contents

Acronyms	iii
1 Introduction	1
2 Method	4
2.1 Literature Review	4
2.1.1 Context	4
2.1.2 Screening Process	5
2.2 Design & Testing	6
2.2.1 Context	6
2.2.2 Tools	6
3 Additive Manufacturing of Self-Sensing Materials: A Review	8
3.1 Additive Manufacturing Of The Sensor	8
3.1.1 Continuous Carbon Fibre (CCF)	9
3.1.1.1 Fabrication	11
3.1.1.2 Curing	12
3.1.1.3 Fibre Extrusion	14
3.1.1.4 Cutters	17
3.1.1.5 Contacts	20
3.1.2 Carbon Nanotubes	20
3.1.2.1 Filament Fabrication	22
3.1.2.2 Single-Wall/Multi-Wall carbon nanotubes	23
3.1.3 Conductive Thermoplastics	24
3.1.3.1 Fabrication	25
3.1.4 Conductive Ink	25
3.2 Additive Manufacturing Platforms	26
3.2.1 Robotic Arms	28
3.2.2 Planar Printers	31
3.2.3 5-Axis Printer	35
3.2.4 Ink Based Printers	37
3.2.5 Discrete Sensor Pick-And-Place (P&P) Machine	37
3.2.6 Nozzle	38
3.3 Software	40
3.4 Literature Review Conclusion	41
4 Manufacturability Analysis	42
4.1 Filament Test	43

4.2	Extrusion Tests	49
4.3	Non-Planarity	53
4.4	Conclusion	55
4.4.1	Materials	55
4.4.2	Manufacturing Method	56
5	Design	57
5.1	Material	59
5.2	Backing Plate	60
5.3	Fibre Spool	62
5.4	Fibre Extrusion	64
5.5	Feeding of CCF	65
5.6	Feeding of Thermoplastic	66
5.7	Cutting of CCF	67
5.8	Software Design	67
5.8.1	Slicing	67
5.8.2	Continuous Fibre Placement	68
5.8.3	Non-Planarity	69
5.8.4	Stepper Motor Logic	70
5.9	Future Work	71
6	Conclusion	73
A	Filament Test Piece	81
B	Backing Plate	82
C	Easy Print Fan Case	83
D	Continuous Carbon Fibre Spool	84
E	Fibre Cutting Arm	85
F	Continuous Pathing Cube	86
G	Ender 3	87

Acronyms

ABS	Acrylonitrile butadiene styrene 23–25
CAD	Computer-aided design 6, 57, 64, 66
CCF	Continuous Carbon Fibre i, ii, 4–6, 8–20, 28, 31–34, 36, 40–45, 47–53, 55–57, 59, 60, 62–69, 71, 73
CFRTP	Carbon Fiber Reinforced Thermoplastic iv, 4, 9, 10, 12, 15, 20, 27–29, 35, 40
COTS	Commercial-Off-The-Shelf iv, 4, 9, 11, 13, 20, 22, 24, 25, 31, 34–36, 41, 42, 49, 53, 57, 59, 64, 66, 73
DW	Direct Writing 23, 25, 28, 36
FDM	Fused Deposition Modeling 1, 6, 8, 12, 16, 20, 21, 23–28, 30, 31, 34, 37, 38, 40–42, 56, 71–73
G-Code	Geometric Code iv, 2, 6, 26, 30, 31, 34, 40, 42–47, 53, 54, 56, 58, 66–69, 73
LDM	Liquid Deposition Modeling 21, 23
LTU	Luleå University of Technology 6, 72
MEMS	Microelectromechanical Systems 37
P&P	Pick-And-Place i, 26, 37, 42
PBT	Polybutylene terephthalate 20, 39
PCL	Polycaprolactone 24
PLA	Polylactic Acid 9, 11, 20, 23–25, 35, 42, 43, 45, 47–55, 59, 64, 65, 67, 69, 73
PP	Polypropylene 23, 40
PTFE	Polytetrafluoreten 31, 39, 40, 49–51, 57, 62, 64–67
PVA	Polyvinyl Alcohol 40
SLA	Stereolithography 25, 31
TPU	Thermoplastic polyurethane 20–23
wt%	Percentage By Weight 20, 42

Abstract

A self-sensing material can not only carry a load but can also provide data about the load and stress it's being subjected to. Traditional additive manufacturing has limited capabilities in producing self-sensing material. Existing 3D printers either used in industry or in scientific applications are either limited by closed-off software and planar motion which limits the design freedom, or the type of material or cost often limiting the attainability. Being capable of placing self-sensing material with full design freedom means that the sensor structure as well as the load carrying part of the material can be tailored to the application specific use of the material, making application specific load carrying and sensing capabilities possible. The manufacturing method produced in this aims to solve these existing limitations. A literature review in the topic of additive manufacturing of self-sensing material and continuous Carbon Fiber Reinforced Thermoplastics (CFRTPs) has been produced as a literature base. The review seeks to educate and inspire the design of an novel additive manufacturing method and device capable of printing a self-sensing material as well as non-planar motion. A design for extruding self-sensing material and non-planar motion has been realized through modified Commercial-Off-The-Shelf (COTS) parts and Geometric Code (G-Code). Existing hardware capable of producing this can be priced in the range of 70 000 €, but this result has been achieved with around 200 € [42]. A software structure capable of manufacturing the self-sensing material has been produced. Real-world testing in terms of extrusion of the self-sensing material and non-planar motion has been tested and proven which are the main practical outcomes demonstrating the technological feasibility.

1 Introduction

Additive manufacturing, or 3D printing can be used to create parts with full design freedom, low material waste and low cost. The additive manufacturing of conductive piezoresistive materials for the application of strain sensing has been a research topic with an increase in recent publications. Strain sensing materials can broadcast their health to the user, a topic that will be further covered throughout the thesis. The goal of this thesis is to produce an end-to-end design capable of manufacturing the self-sensing material, together with a literature review as the basis for the design. A piezoresistive material can change in resistivity in a predictable way when it experiences strain, this characteristic is what can give a material strain sensing properties. When a change in resistance of the piezoresistive element is measured within the material, through electrical contacts it can be correlated to a change in strain which makes the analysis of forces and deformations that the material is experiencing possible. Having a material be self-sensing means that it can broadcast its health to the user in ways that could not be achieved otherwise without adding sensors into it, traditionally done by gluing strain gauges to the outside of the material, which could compromise the structure and limit the use to scientific testing in a lab rather than practically in the field. This thesis aims to produce a novel additive manufacturing process for self-sensing materials. The product will take heavy inspiration from existing state of the art research and technologies, and aims to solve existing manufacturability issues. An example of an end-to-end manufacturing process for creating, additively manufacturing and applying carbon nanotube doped thermoplastics to self-sensing scoliosis braces can be seen in Figure 1.

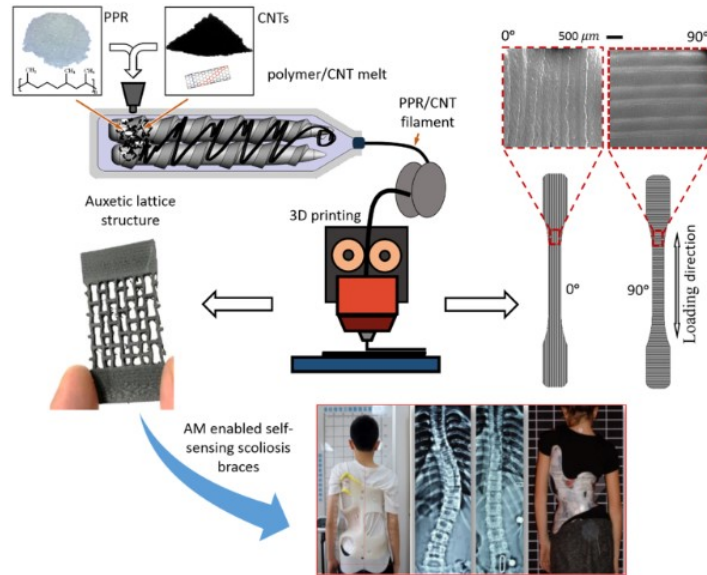


Figure 1: Filament fabrication and Fused Deposition Modeling (FDM) of a thermoplastic with carbon nanotubes as the piezoresistive element. Development of individually tailored biomedical devices, such as scoliosis braces [62, 64].

Parts that are traditionally given an expected lifetime can also, or instead notify the engineer, company or hobbyist that it may need changing due to deformation, or that an unexpectedly high force has been experienced [40]. A traditional scoliosis brace would have to have higher margins accounting for the uncertainty of not being aware of the degradation of the part, or have external sensors attached onto it to produce the strain sensing data. Having this information means that the failure of the part can be foreseen and prevented before it occurs, or provide the user with data about the cause of failure in order to engineer the next part to be more reliable and combat against the failure modes experienced by the material. When building parts for a car, a CubeSat, an end effector for a robot arm, or other parts which are meant to handle vibrations and forces, the prototyping and engineering samples of the parts may need to be stress tested. Stress testing involves subjecting the part to stress until it fails, or until a threshold is measured. If a self-sensing material would be applied for the prototype or engineering sample, not only could the material give the data needed for the stress test but also have the same prototyping material with sensors be the actual part that gets put in use rather than going from a part with external sensors to no sensors, which is a reason for using additive manufacturing to produce the material. Additive manufacturing is also a way of providing a high level of automatization and a high degree of design freedom for application specific structures and sensor structures [50] that can be developed with the addi-

tive manufacturing device that will be designed and defined in this report. Tool path optimization through G-Code manipulation can make almost any sensor structure possible to manufacture, for example placing continuous fibre filament through continuous material placement paths. Or even having traditional 3D printers move at an angle to the plane when printing in something called non-planar printing.

The contents of this thesis will include a literature review into the additive manufacturing of self-sensing piezoresistive materials. The literature review will provide an overview of what methods, platforms, materials and existing designs are used. The capabilities to manufacture the material will be analysed, and through that manufacturability analysis a design path will be taken. It involves deciding what material, printing method, and printing platform should be used to realize novelty and functionality for both the manufacturing device and the resulting part. Novelty factors will be identified and the design of a novel 3D printer designed to print the self-sensing material will be provided together with justifications for the manufacturability of the material with the 3D printer.

2 Method

The method for real-world implementations, testing, design and software have been based off the literature review. Defining what literature is of interest and how to keep track of it had to be determined.

2.1 Literature Review

For the literature review a literature base had to be generated. A method for finding literature and patents that were consistent with the main topics of focus had to be determined.

2.1.1 Context

Existing benchmarks and research in the field of additive manufacturing of self-sensing materials and the properties of the structural and sensor material has been generated which will aid the development of the additive manufacturing method, hardware and software. The literature will provide a basis and justifications for design decisions and explore what patents exist and what companies are doing. Seeing what combinations of functionalities paired with manufacturing designs and materials have not yet been implemented will be a focus of the review as well, through which novelty could be realized. The search terms varied as a result of other literature, and the references within that literature. The main topics remained the same and are as follows.

1. Additive Manufacturing of Self-Sensing Materials
2. Additive Manufacturing of Materials:
 - (a) CCF
 - (b) Carbon Nanotubes
 - (c) Conductive Thermoplastics
 - (d) Conductive Inks

Another purpose of the literature review is to consider design methods used by researchers regarding the additive manufacturing of self-sensing materials and continuous CFRTPs, and what trade-offs are made by picking the various design methods. What trade-offs are made when for different designs, and at what cost or gain. Designing a highly customized system will likely perform very well at the task, but may require a lot of time, complex systems, expensive manufacturing methods,

custom software and more. It's not a guarantee that it would perform better, and the time commitment into making a custom highly engineered system may not be worth it. On the other end of the spectrum seeing which researchers went with a COTS inexpensive system and modifying it to be able to meet the requirements for producing the part, as opposed to having a highly custom system fabricating more of the design in house. Through benchmarking of existing solutions the design philosophies commonly used for the manufacturing of self-sensing materials and continuous CFRTs will be considered, which will serve as an inspiration for what to make custom, and what not to.

2.1.2 Screening Process

A mix of state of the art widely publicised research combined with some more in depth and niche research provide important benchmarks for the design helping to create a literature base. The literature base was generated through *Google Scholar*, *Google Patents* and *Scopus* throughout the review. A flow chart explaining the screening process can be seen in Figure 2.

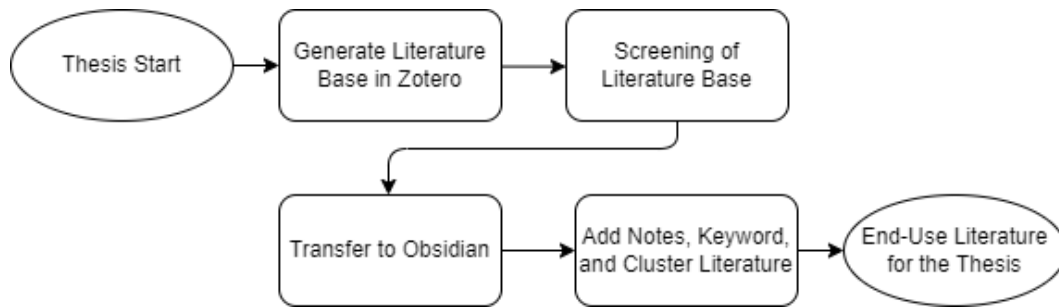


Figure 2: A flow chart explaining the largest parts of the screening process.

Initially a lot of the literature was reviewed very roughly and saved in a reference manager, *Zotero*. Once sufficient literature had been produced less relevant articles get screened out through a rougher screening process and possible duplicates removed. The screening stage removed references that did not mention additively manufactured sensors or CCF's. An important note is that essentially all documents that only mention the science or application of the sensors were removed since the relevancy lies in the additive manufacturing of the self-sensing material, and literature complementary to that. Wherever science and application was to affect the additive manufacturing method, it could be seen as complementary literature. After a screening process, the remainder of the literature was screened again and grouped into categories marked with keywords in a note organizing software, *Ob-*

sidian. From this a clear picture of the distribution of literature, when it comes to the amount of benchmarks, amount of the different materials, amount of manufacturing platforms, different use cases and more was identified. In other words the data was clustered generating not only statistics but a way to find information and sources by accessing a category or keyword. The final screening involved extracting sources from the database while others remained unused. The process, as described above, of going through multiple screenings with an increasing level of detail was inspired by the Preferred Reporting Items for Systematic Reviews and Meta-Analyses (PRISMA) workflow, even though it has not been strictly followed.

2.2 Design & Testing

For making the design, hardware and software tools to use has to be determined. All of these design aiding tools have to be weighed against other tools available. There are numerous Computer-aided design (CAD) software's and numerous G-Code editors. There are numerous ways to modify hardware that can produce the same quality in the end, so the most practical methods have been the focus.

2.2.1 Context

The hardware, software and tools can be chosen freely depending on what is recommended through literature and what is available through Luleå University of Technology (LTU), Kiruna, either through software licensing or lab hardware. Drill presses and various ways to cut parts have been used which will be explained further. Availability of hardware and software is not certain, so it is a significant criteria as well. Some tools have to be purchased and some are available through LTU, and these have been weighed against each other for the sake of cost, time and ensuring design feasibility.

2.2.2 Tools

Software's used for the design were *SolidWorks 2021* for the CAD models and blueprints, making the part which should be printed. It's also required to generate and modify G-Code, which is code that a 3D printer can read which mainly communicates stepper motor commands and extrusion motor commands needed to move the end-effector in space and control the flow of thermoplastic through the nozzle. The generation of the main bulk of the code is done through slicer software, in this case *Ultimaker Cura 4.11.0*. Modifying the G-Code just means modifying text files, so a text editor of any kind is capable of doing it but in this case *Notepad++* has been used together with *Repetier-Host 2.2.4* to modify G-Code. *Repetier-Host*

2.2.4 has a G-Code viewer as well making it convenient for analysing the changes in G-Code and is mentioned in literature for scientific applications [66, 40, 38]. A script capable of implementing non-planarity for a traditional FDM 3D printer has been used [10]. Hardware available and used for testing the manufacturability of the self-sensing material as well as a design basis is the *Creality Ender 3* 3D printer, which is modified to be capable of additively manufacturing self-sensing materials. CCF tows have been used as the material when testing and designing the manufacturing process.

3 Additive Manufacturing of Self-Sensing Materials: A Review

The main areas that will be reviewed with regards to the topic will be the additive manufacturing of the sensor Which is the piezoresistive element of the self-sensing material. Here the method of producing the material will be covered as well, which includes the way it is extruded and placed. The manufacturing platform which is used to hold and control the print head which extrudes the self-sensing material. As well as the software required and generally used for the additive manufacturing of self-sensing materials.

3.1 Additive Manufacturing Of The Sensor

The sensing parts of the self-sensing materials have to be electrically conductive in order for measurements to be taken. Being conductive is not enough for materials to provide sensing data, the material also has to be piezoresistive which means that the resistance changes when a pressure or force is applied. Several piezoresistive materials capable of being additively manufactured were found in literature. These materials are CCF, conductive thermoplastics, which are thermoplastics combined with a piezoresistive element, carbon nanotube's, which are added to thermoplastics or inks, or inks on their own with various piezoresistive elements. Depending on the material different feeding and extrusion methods generally had to be utilised. If the material that was being fed were to be a thermoplastic combined with piezoresistive materials, a fairly normal FDM method could be used. However, designs using CCF's extruded in a thermoplastic matrix may need a different feeding mechanism due to things like fibre flexion and a possible need for cutting capabilities to stop the continuous fibre extrusion. The spread of materials utilised in literature can be seen in Figure 3.

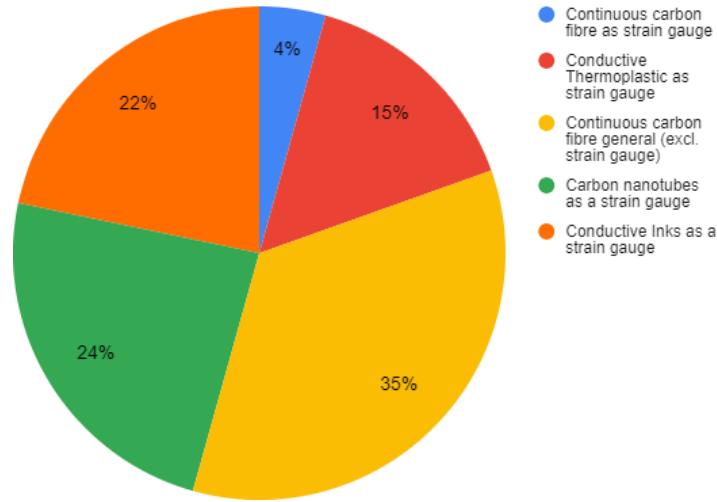


Figure 3: Pie chart showing the distribution of the manufactured materials in the literature count, which includes papers and patents.

The additive manufacturing of self-sensing materials involve a structural and insulating material which help build up the geometry of the part. A piezoresistive component is used to generate the electrical connection through the material so that the change in resistance over that length of sensing material can be measured. Together the combination of structural material and piezoresistive material create the self-sensing material.

3.1.1 CCF

Continuous CFRTP parts have been additively manufactured for scientific purposes but also for industry. Companies such as *Markforged* have been able to reliably print continuous CFRTPs, for which they have some active patents [42]. The printing has been realized in several ways from having in-nozzle impregnated fibres with COTS extrusion mechanisms [45, 50] to dual extrusion using highly customized end effectors [40, 42]. A highly retrofitted design where an existing COTS 3D printer gets modified to be able to additively manufacture CCF reinforced Polylactic Acid (PLA) has been shown to be viable [66]. Articles related to the use of CCF as a sensing material [41, 66] is more inline with what the design seeks to accomplish. However, literature where additively manufactured CCF is used a structural component can still provide methods and designs for printing the fibre. That means that literature relating to either of the two is relevant since the piezoresistivity of the CCF's remains for both use cases. The widespread use of additively manufactured CCF through either custom or retrofitted designs in litera-

ture means that the capability to produce the material is not limited. The structural component of the self-sensing material using carbon fibre as the sensor was generally comprised of thermoplastics. The focus of the literature review has not been on the structural material, but throughout the analysis the materials used with the sensors have been identified. Being able to change the directions of the CCF's means that omnidirectional strength can be achieved. Which means that the material has improved mechanical performance in all directions. Targeted strengthening of the material can also be achieved where the fibres are oriented in a way that combats the expected stresses [69, 50]. Selective reinforcement is another process that can be used which aims to add fibre to highly stressed areas while less stressed areas can be supported with just the thermoplastic matrix or a smaller amount of CCF. An illustration of fibre placement that combats the use case specific loads can be seen in Figure 4.

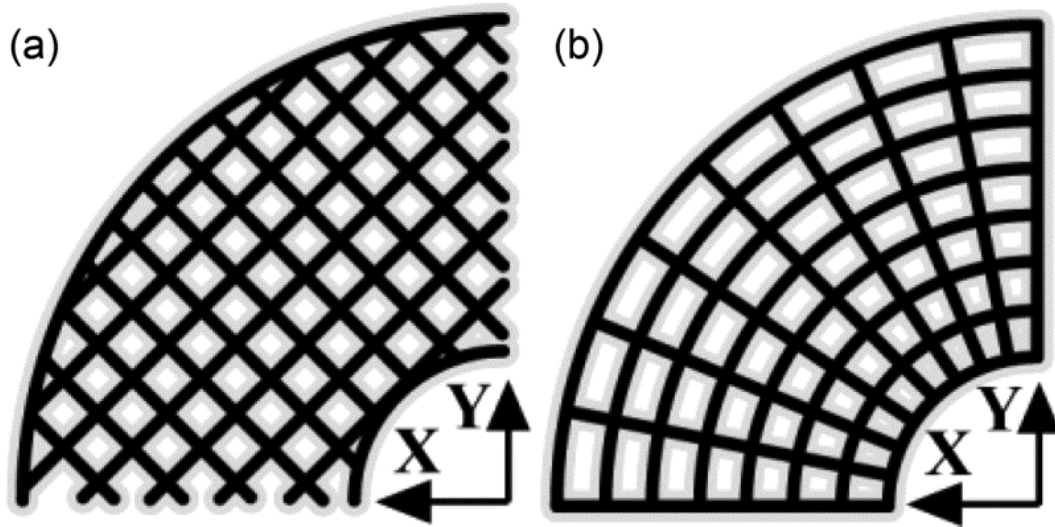


Figure 4: Infill: (a) Generic 3D printer slicer pattern (b) Pattern to resist a specific load direction. [50].

An overwhelming majority of sources using additively manufactured CCF has done so for scientific purposes testing the material properties. But the capability of additively manufactured CCF for real world use cases has been proven as well, as in an example where It's being used in aerospace structures [17]. A summarization of different levels of geometrical complexity of additively manufactured continuous CFRTs is shown in Figure 5.




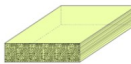
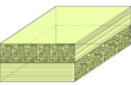
Specimen Complexity	Manufacturing	Electrical connection material	Electrical connection position
I: Single fiber 	Surface polished	Sputtered	Top Surface
II: Embedded fiber 	Surface etched	Galvanized	Lateral Surface
III: Embedded roving 	Elevated temperature cure	Silver epoxy	Cut end
IV: Unidirectional laminate 	Prestressed	Silver paint	Electrical measurement
V: Multidirectional laminate 	Poststressed	Carbon cement	
	Embedded in GFRP or polymer	Mechanically clamped	
	Prepreg / Dry fiber		2-wire
	Fiber volume fraction		4-wire
	Fiber waviness		Wheatstone Bridge

Figure 5: Summarization of different experimental configurations used in the past for the evaluation of self-sensing additively manufactured CFRTPs. [54].

The figure shows geometries used for the demonstration of the self-sensing technology, rather than applied designs. But the geometries are still the same or similar to what a functional part would use. Different types of additively manufactured CCF reinforced plastics can be seen in an increasing level of complexity, as well as properties that the CCF's can add to the thermoplastics. Suggestions on the manufacturing of the self-sensing material are mentioned as well as the electrical connection commonly used for the validation of piezoresistivity.

3.1.1.1 Fabrication Obtaining CCF is an feasible as there are many online retailers capable of shipping CCF tows. The tows come in varying filament counts, generally a few thousands of filament in one tow, denoted as 3K, 6K, 12K and so on where the number before the K says how many thousands of fibre's there are in one strand of tow. The number of fibre's directly correspond to the width of the tow since fibre's generally have the same diameter. Sizing of the fibre can be performed resulting in CCF's tows generally having a diameter of $7\mu\text{m}$ at COTS CCF tow retailers [8]. Additive manufacturing capabilities have been shown for filaments such as T300B-3000-40B Torayca for a dual extrusion print head [40, 41, 66] which also utilises a cutter for cutting the CCF filament together with PLA thermoplastic. T700SC-6000-50C, and T700SC-12000-50C have also been utilised for

evaluating the functionality of self-sensing characteristics of CCF through additive manufacturing [66]. The property which gauges the capability to act as a sensor is the gauge factor, different CCF's generally have different gauge factors. Several types of CCF with varying gauge factors and modulus can be seen in Table 1.

Table 1: Different CCF filament's utilised for their piezoresistive characteristics, based off table in a review [54].

Manufacturer	Fibre name	Filament Count	Gauge Factor	Source
Toray	T300	1K	1.71	[25]
Toray	T700SC	12K	2	[26]
Toho Tenax	HTA40	1K	1.72	[23]
Toho Tenax	T300B	1K	1.54	[23]
Nippon	PAN based	6K	2.85–3.36	[65]
unspecified	PAN based	24K	1.35	[51]
Toho Tenax	HM35	12K	1.96–2.17	[31]
Toho Tenax	T300B	3K	1.5	[41]

The filament counts used for self-sensing vary highly from 1K to 24K, showing that many different CCF tows can be used. Even though the data interpretation of the sensor is not relevant to the capability of CCF printing, the choice of filament can still affect the manufacturing process. The varying modulus affects the gauge factor and the capability for the CCF tow to act as a sensor, a large modulus which has a better degree of extrusion capability due to higher rigidity generally makes the gauge factor go down [54].

3.1.1.2 Curing A consideration when producing additively manufactured parts with CCF is the option of curing of the fibre. Curing when related to CCF is a process of bonding a thermoplastic or thermoset to dry CCF. The thermoset or thermoplastics that can be used can be epoxy, polyester or vinylester which changes the properties of the fibre to a more structurally viable material [8]. For the additive manufacturing of CCF, curing is generally done manually to reduce the complexity of the CCF printer. Since most literature revolves around scientific tests of the additively manufactured continuous CFRTs, having another layer of complexity is likely not relevant. Curing of dry CCF during printing can also be done through manually adding thermoset epoxy powder mid-print [69]. There are several different methods of integrating the curing of CCF in the additive manufacturing process, several of the methods used and theorized are summarized in Figure 6.

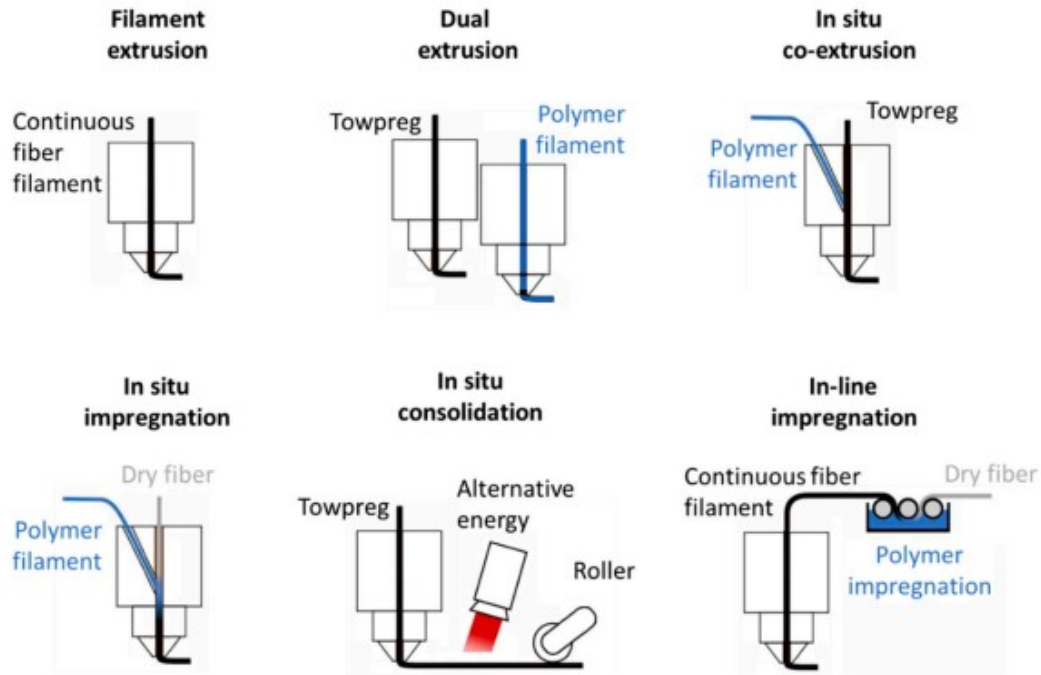


Figure 6: Curing and extrusion of additively manufactured continuous CFRTs through FDM classified by increasing complexity. [43]

For fibres of with different categories of pre-impregnation seen in the figure, the method of even further impregnation is shown in Figure 6. Even the case of going from a dry fibre to an impregnated fibre. The extrusion of the CCF can utilise COTS hardened nozzles to extrude the fibre reliably [17]. Pre-impregnated CCF can be integrated into the structural material either through extrusion via the same nozzle as the structural material or by extruding the fibre's and the thermoplastic separately where the thermoplastic gets printed on and around the fibre. In situ impregnation of the polymer filament with dry fibre could give the possibility of varying the fibre's exposure to the thermoplastic, leaving contact points for the CCF sensor where the insulating polymer would not cause as much electrical impedance [3].

Being limited to for example *Markforged* printers only capable of using the company provided CCF filament limits the possibilities to utilise different CCF's. It's pre-impregnated with a thermoplastic which may cause electrical impedance [44]. In-line impregnation means that curing can be separate from the integration of the fibre and the thermoplastic filament, but requires another manufacturing step and system outside the print head impregnating the CCF [43]. The concept of in situ consolidation has been actualized through a dynamic capillary-driven method of

additive manufacturing of CCF using a robotic arm and a heating element to melt epoxy resin onto the placed fibre's [56], the process can be seen in Figure 7.

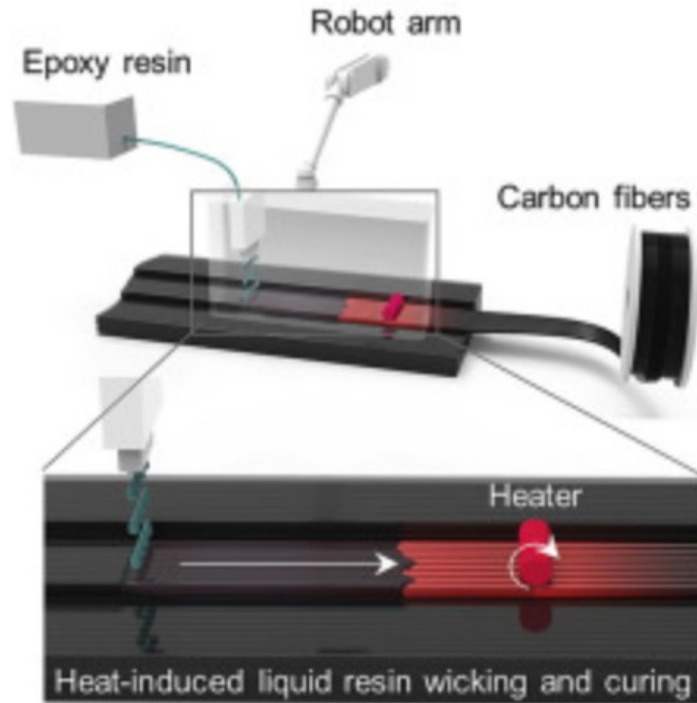


Figure 7: Design schematic showing the in situ consolidation in the additive manufacturing of CCF [56].

3.1.1.3 Fibre Extrusion Issues such as fibre snagging can be a problem when extruding CCF, where the fibre gets stuck, gets snagged and likely breaks [13]. Tensioning of the fibre is important to keep a consistent and reliable fibre flow all the way from the fibre spool to the nozzle. A patented feeding and extrusion design with two stepper motors can be seen in Figure 12 where two rollers actuated by the stepper motors extrude the fibre. A nylon sizing agent can be included in the feeding process, which is a tool to increase the reliability of curing by modifying the surface of the carbon fibres for better adhesion with thermoplastic or thermoset.

The extruder driver is the fibre feeding mechanism of the printer and drives the fibre to the nozzle. It has the fibre as an input which continues its way to the nozzle and then the print bed. Heating of the nozzle for the extrusion of CCF can be relevant if the structural thermoplastic is extruded through the same nozzle through in situ curing or adhesion. Pre-heating the fibre can prevent the fibre from cooling down

the thermoplastic when entering the nozzle. A completely custom fabricated end effector with the flow of resin and CCF visualized can be seen in Figure 8 [38].

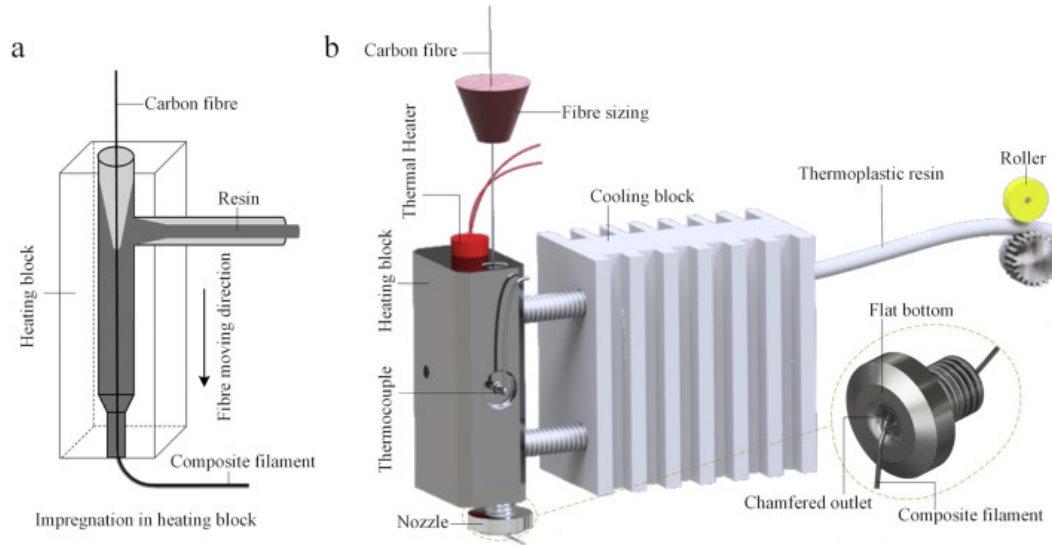


Figure 8: (a) Impregnation diagram of carbon fibre and resin matrix, (b) Illustration of the printing head [38].

Dual extrusion configurations can be used to produce the same result as a single nozzle configuration with the added benefit of being able to cut off the CCF while still extruding the thermoplastic, or stop the extrusion of thermoplastic while still extruding the continuous fibre. Configurations which include a manual lay up of epoxy resin and a curing agent has been implemented to complement the additive manufacturing of CCF for structural applications [66]. However, a lay up method is not additive manufacturing of the CCF, but rather combining CCF lay up to additively manufactured parts. As mentioned, a method of impregnating continuous CFRTs through pure additive manufacturing and adhesion to thermoplastic using in situ curing of the CCF in the nozzle has been implemented in Figure 8. Using in situ curing is a method frequently used when extruding CCF's, a real-world design based on a patent using pressure to aid in in situ curing has also been implemented [50, 18] which seeks to increase the reliability of the curing and adhesion of the fibre and thermoplastic. A figure of the real-world in situ curing nozzle can be seen in Figure 9 where the extruded CCF can be seen flowing through the nozzle.

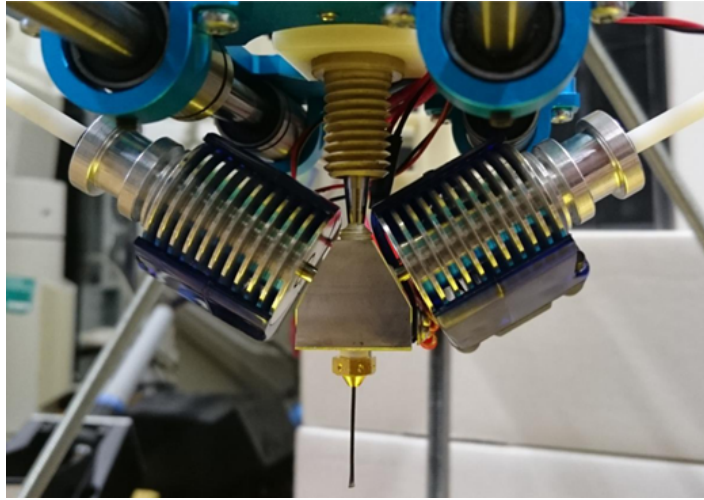


Figure 9: In situ curing with the extruded filament visible [50].

The principle that the patented in situ curing design followed is based on a patent on the extrusion of elongated fibre strands with low rigidity such as CCF or plastic fibre [18]. Thermoplastic wets the continuous fibre on its path from the filament holder to the nozzle with a pressure at the thermoplastic contact zone that helps keep the fibre extrusion controlled. The patent drawing can be seen in Figure 10 and the clear inspiration can be seen between the real world design in Figure 9 and the patent in their shape.

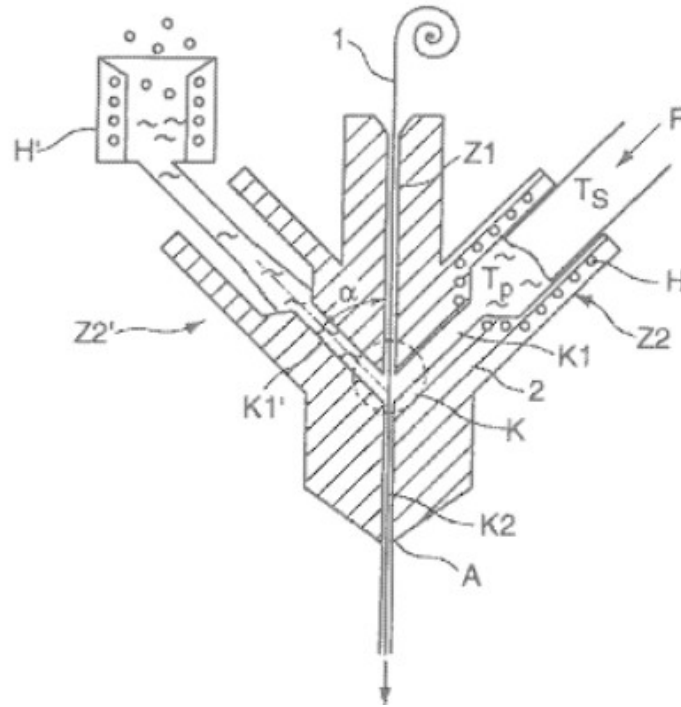


Figure 10: Prototype of an adapted FDM print head for the printing of elongated fibre strands [18].

When using a single nozzle to extrude both CCF and thermoplastic, the adhesion of the fibre and thermoplastic will occur naturally, but with the added pressure from the gaseous substance denoted by H in the figure, the reliability of the bonding between the fibre and thermoplastic or thermoset can be improved. Another point in the design is that the thermoplastic impregnated CCF gets extruded with the help of friction between the thermoplastic and the CCF. The friction provides anisotropic lengthwise tension in the CCF reducing the probability of failure in the extrusion of the fibre often seen in the form of buckling and fibre snagging. Buckling is when the fibre starts twisting or balling together while fibre snagging is the fibre getting stuck and breaking.

3.1.1.4 Cutters Since the fibre is continuous a way of starting and stopping the extrusion needs to be added, either through dual extrusion printers or the utilisation of cutters. Cutters are commonly utilised for the additive manufacturing of CCF's [40] [41] [53] [42]. Since the goal is to have segments of carbon fibre in specific areas of the structure, either for sensing purposes or reinforcement purposes there needs to be some way of interrupting the extrusion of the CCF. One way of cutting

is to have a sharp edge driven by a motor to make a cut at the nozzle, which is something utilised by a design patent seen in Figure 11 to cut pre-impregnated fibre[44]. The object with the number 8 is the cutter, and 12 is the backing plate.

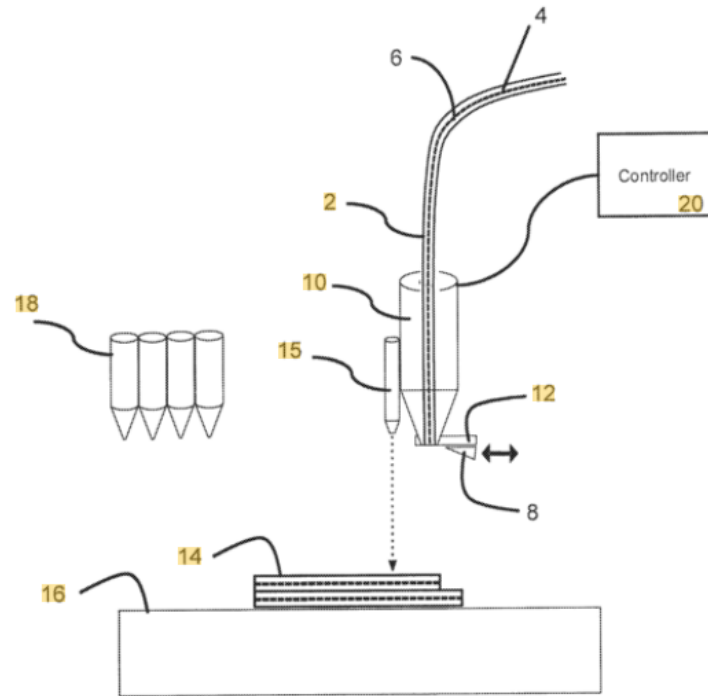


Figure 11: Nozzle and extrusion apparatus for additive manufacturing of CCF [42].

Integrating cutters reliably requires precise engineering, control and software integration. Which is a weakness of utilising CCF. By placing the cutter inline with the feeding mechanism an advantage of not having the cutters obstruct the print head can be achieved. A way of doing it is inducing a cut in the material at a specific point which then creates a weak point in the filament which can later be pulled to break at that that exact spot. A design patent for a system utilising that can be seen in Figure 12.

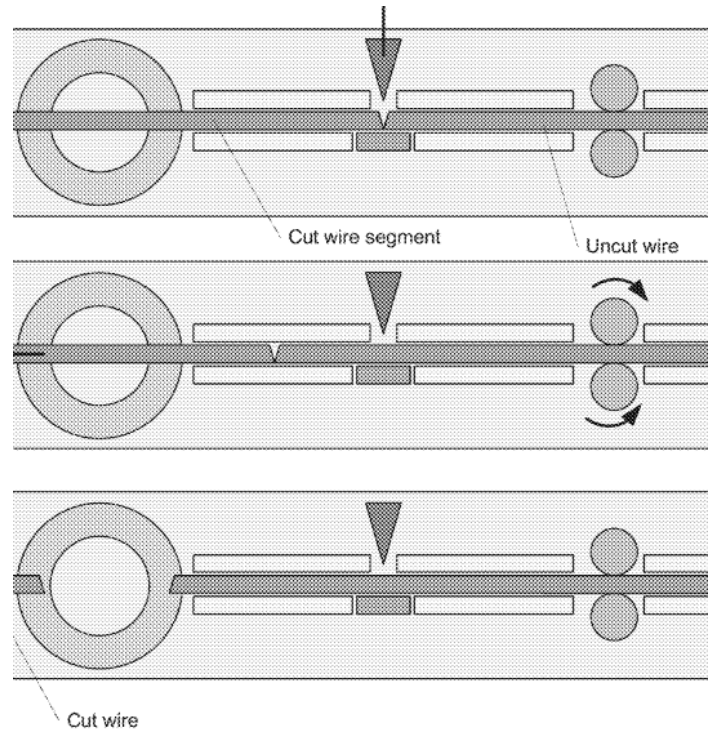


Figure 12: Apparatus for inducing a cut in continuous material [11].

An issue with the previous design would be the compatibility with fibre tows. Since there's no mechanical bond in dry CCF between individual fibre's, the cutter design can not be applied on dry CCF tows. Implementing the cutter on a fibre tow could result in some of the fibres snapping and some staying rigid. Individual fibre's that get pulled may also separate from the carbon fibre tow which is only kept together by a slight friction between the fibre's. One or more of the fibre's could start to traverse lengthwise with respect to the other fibre's.

Due to the flexibility of dry CCF there issues such as buckling could arise when the fibre's get fed into the nozzle, especially if the carbon fibre tow is cut while printing which would leave one of the ends loose. When the fibre gets cut it will lose most of its tension. Reliability of the CCF to nozzle feeding is thought to be highly affected if the filament was cut, or even break during printing. Getting the fibre's back into the nozzle or feed line can be difficult once one end is unsupported. Having tension on the fibre should be done wherever possible. Another option is having a dual extrusion configuration with the nozzle's being able to move individually allowing a structure of CCF to be placed throughout the material without cutting of the fibre's [41]. With a concept called lattice printing which involved moving the

nozzle vertically at the same time as in the plane providing a non-planar printing motion means that having the fibre's move up to the next measurement point is possible as well [63].

3.1.1.5 Contacts The contacts for the CCF needs to be accessible outside the part where electrical connections need to be made. When contact to the CCF is accessible sophisticated sensor structures can be fabricated. A matrix of contact points embedded into a additively manufactured part as with CCF's as the sensing element can be seen in Figure 13.

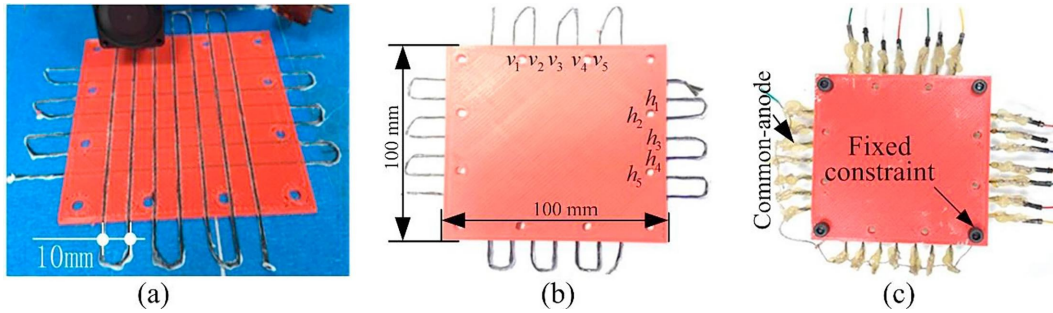


Figure 13: (a) Real printing process. (b) The final printed CCF reinforced PLA matrix. (c) The final self-sensing structure after adding as contacts [40].

The only industrial grade commercial 3D printer's found to be capable of producing continuous CFRTs such as the *Markforged* printers were not capable of placing contact points for the sensor structure outside the material. The lack of ability is mostly due to closed off-software, but the printer is also constrained to only printing the fibre supplied by the manufacturer [44].

3.1.2 Carbon Nanotubes

Carbon nanotubes are commonly used as the sensor for additively manufactured self-sensing materials. Their piezoresistivity joined with the ability to lace several thermoplastics and materials with the nanotubes make them a versatile additive that can be extruded with a similar level of success to thermoplastics while still providing strain sensing and conductive properties for the material, even reaching strain gauges of 176 [9]. By combining multi walled carbon nanotubes with commonly used thermoplastics such as PLA an increase of the electrical conductivity from 0.1 S/m to a range of 10 S/m to 100 S/m could be achieved [49]. The increase in range was due to a multi walled carbon nanotube doping of 5-10 Percentage By

Weight (wt%), which follows the percolation behaviour with a percolation threshold of 0.67 wt%. The value of wt% is an important parameter to take into account in the material manufacturing of carbon nanotube doped thermoplastics due to higher levels of carbon nanotubes possibly altering the viscosity and the dispersion quantity of the material which then has to be extruded [5].

Carbon nanotubes can be printed with modified FDM COTS 3D printers and the technological feasibility has been demonstrated by printing polymer nanocomposites (carbon nanotube- and graphene-based Polybutylene terephthalate (PBT) [20]. The method of overcoming extrusion inconsistencies was by optimizing the conductive filler sizes and printing parameters and conditions. These can be the printing temperature, printing speed, printing bed temperature and residence time. A printing configuration utilising a dual nozzle configuration with the *Makerbot 2X replicator*, USA where one nozzle's extrudes structural material and another nozzle extrudes a carbon nanotube/Thermoplastic polyurethane (TPU) blend can be seen in Figure 14.

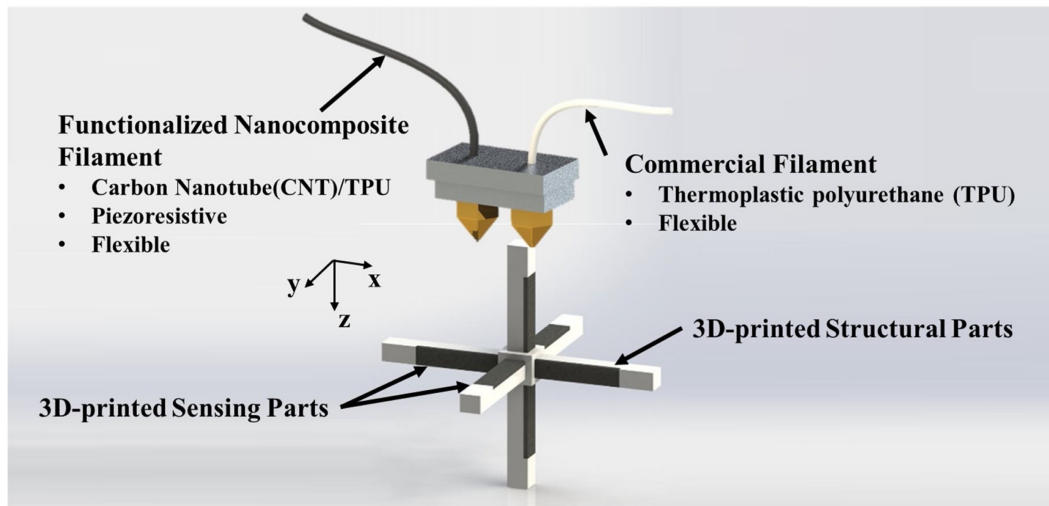


Figure 14: Design of a 3D-printed multi-axial carbon nanotube and TPU force sensor and fabrication based on the simultaneous FDM type 3D printing of self-sensing and structural materials [33].

The feeding and extrusion of carbon nanotubes is generally done through traditional FDM 3D printing. But the possibility of utilising Liquid Deposition Modeling (LDM) printing for the printing of carbon nanotube doped thermoplastics has been found to be viable as well, which makes the additive manufacturing of carbon nanotubes more versatile [49]. The abrasion caused by carbon nanotubes means

that the nozzle and parts that are directly exposed to the melted filament needs to be abrasion resistant [20]. The nozzle can easily be changed from the typically nominal brass nozzle into a steel nozzle or other kind of hardened nozzle. More frequent changes of nozzles may still be required.

3.1.2.1 Filament Fabrication Even though there's a large set of literature for the applications of utilising the piezoresistivity of carbon nanotube doped thermoplastics, there are no COTS 3D printing filament available with a transparency from the manufacturer in the amount of carbon nanotubes in the material. This is an area of future work for 3D printed self-sensing materials. Carbon nanotubes likely need to be fabricated through combining raw COTS carbon nanotubes with a thermoplastic melt. The carbon nanotube doped thermoplastic melt needs to be extruded with a highly controlled diameter. Cooling down of the extruded material needs to be done quickly to minimize warping and deformities after the extrusion [33]. On top of the additive manufacturing hardware, hardware for producing the material is required as well. Having a tightly controlled diameter can be difficult for manufacturer's of thermoplastics for additive manufacturing, so a custom solution will likely perform worse. The fabrication method can still be the same as for COTS filaments where additive's for the COTS would be added. A custom designed material manufacturing configuration which yields 1.64 mm filament with a standard deviation of 0.049 mm can be seen in Figure 15.

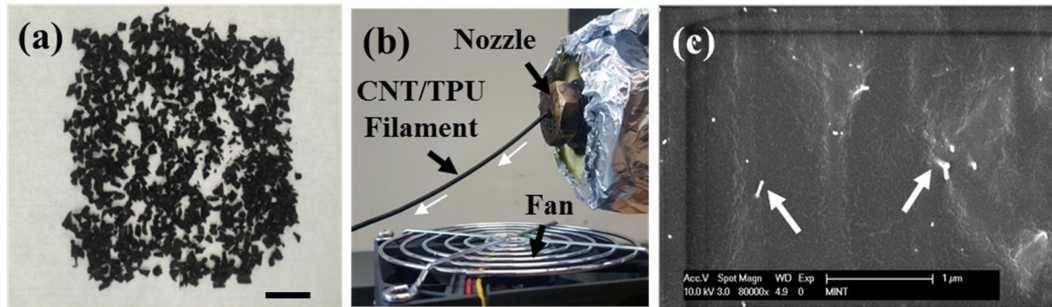


Figure 15: (a) Carbon nanotube/TPU pellets after shear melt process and pelletizing (Scale bar = 10 mm) (b) Extruded carbon nanotube/TPU filament. White arrow indicates the extruding direction. (c) Scanning electron microscope images of carbon nanotube/TPU. The arrows indicate the carbon nanotubes [33].

The inter layer adhesion for carbon nanotubes doped thermoplastics is feasible but still affected when using TPU/carbon nanotube mixes for the sensing, capable of around 60 % of the strain that the pure TPU would be capable of [9]. Due to the

material fabrication having to be customized, the geometrical consistency for the filament may not be sufficient which may cause feeding or even nozzle clogging of the nozzle. The fabrication of the carbon nanotube doped thermoplastics is a large detriment for using carbon nanotubes as the sensing material in the design.

3.1.2.2 Single-Wall/Multi-Wall carbon nanotubes Carbon nanotubes come in configurations of single-wall carbon nanotubes or multi-wall carbon nanotubes. Single-wall carbon nanotubes enable the fabrication of carbon nanotube doped materials with a minimum spatial resolutions of a few hundreds of nm [60, 16]. The fabrication of the sensor can also be done through a process called Direct Writing (DW). An example of DW being used for printing carbon nanotube doped ink can be seen in Figure 16. The configuration utilises several nozzles and the type of additive manufacturing device is an inkjet printer.

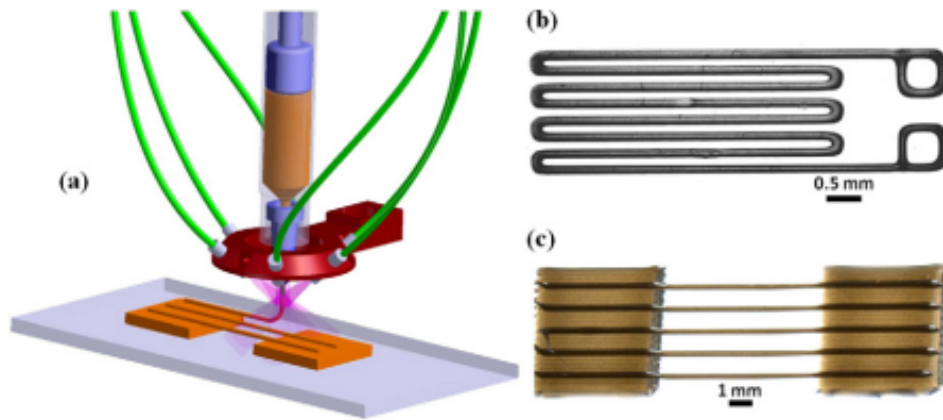


Figure 16: (a) Schematic representation of the UV-assisted DW of the carbon nanotube sensor. (b) A deposited line network similar to traditional strain gauges. (c) Microfiber coupon. To fabricate these microstructures using the UV-DW technique, the sensor material is extruded through a capillary micro-nozzle by an applied pressure and is partially cured shortly after extrusion under UV illumination [16].

Using multi-walled carbon nanotubes for strain sensing is possible as well. The thermoplastic matrix used for the structural material can be composed up of several different thermoplastics. Common thermoplastics used are Acrylonitrile butadiene styrene (ABS), TPU PLA and Polypropylene (PP) which have all shown successful strain sensing capabilities when combined with multi-walled carbon nanotubes. FDM 3D printing has been used in the additive manufacturing of carbon nanotubes using the mentioned thermoplastics [32, 9, 34, 62]. LDM 3D printing has also

been shown to be viable for applying the carbon nanotube doped thermoplastic as a conductive element [49].

3.1.3 Conductive Thermoplastics

Conductive thermoplastics is any thermoplastic that can conduct electricity. The area of interest is specifically the additive manufacturing of piezoresistive conductive thermoplastics rather than just conductive thermoplastics. Carbon nanotube doped thermoplastics fall well within the category of conductive thermoplastics, but will be referenced to as carbon nanotube's in thermoplastic rather than conductive thermoplastics to have a distinction between the categories. Mainly because 3D printing of conductive thermoplastics can be done with a high level of reliability due to the COTS availability and market providing a high level of standardization for the product, which is not the case for carbon nanotubes. Having a material that's commercially viable requires it to be competitive compared to other options. Conductive thermoplastics don't inherently imply piezoresistivity, but many conductive thermoplastics are piezoresistive. There are thermoplastic composites that incorporate carbon-based additives into thermoplastics giving a near linear correlation between resistance change and strain induced in the material [12]. PLA, ABS and Polycaprolactone (PCL) as the thermoplastic matrix laced with carbon black have been demonstrated to have piezoresistive characteristics and can function as a strain gauge under mechanical stress of the self-sensing material [12, 37, 27]. Some COTS thermoplastics with piezoresistive additives that have been utilised as strain gauges are as follows.

- ProtoPasta (Carbon black & PLA) [27]
- Conductive ABS (Carbon black & ABS) [27]
- Carbomorph (Carbon black & PCL) [37]

COTS 3D printers can be used for the printing of conductive thermoplastics without many modifications, often no modifications at all having to be made. That is due to the material being marketed and designed to be compatible with traditional FDM 3D printers [48, 47, 37]. The printer likely has to be outfitted with a second nozzle so that structural material and sensing material can be isolated from each other [21]. If there were to be no isolating material between the piezoresistive elements the entire material would be sensing the strain instead of localized strain sensing. Conductive thermoplastics need to be complemented with non-conductive structural materials to work as discrete sensors. An illustration of the polymer matrix and the conductive path with isolation that is required can be seen in Figure 17.

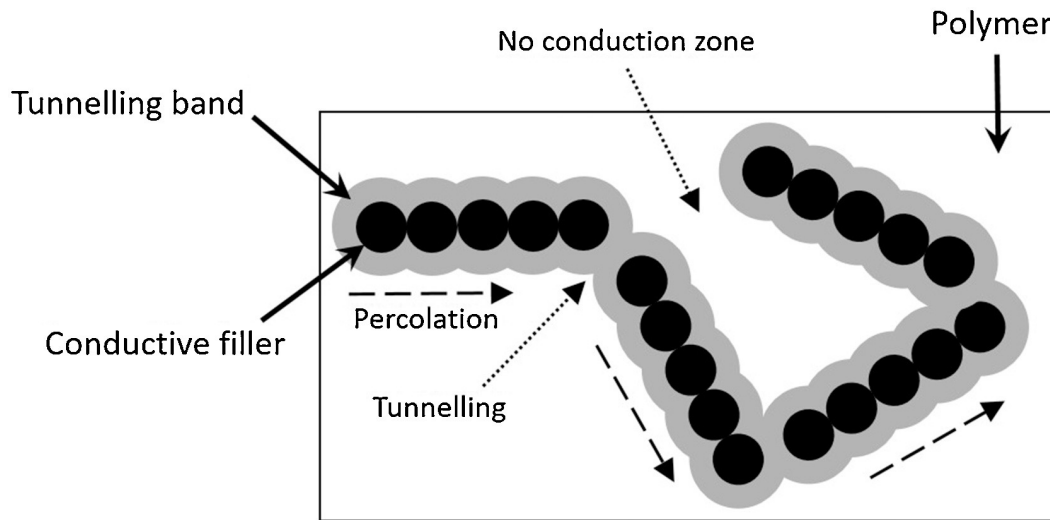


Figure 17: The tunnelling and percolation conduction mechanisms [12].

Percolation happens when the conductive additive touches the surrounding conductive additive creating a conductive network. Tunneling occurs when electrons have to traverse an insulating element which increases the resistance of the connection. These characteristics cause the material to be piezoresistive.

3.1.3.1 Fabrication Carbon black is the most frequently used additive in the fabrication of conductive thermoplastics. It's produced through the incomplete combustion of heavy petroleum products. Conductive PLA often goes by the name of ProtoPasta and is available as a COTS product. Carbomorph and ProtoPasta differ in their electrical conductivity and ProtoPasta has been shown to have an electrical conductivity that's 56% higher than Carbomorph [27]. ABS thermoplastics are generally more difficult to print than PLA thermoplastics. ABS often requires a temperature controlled environment and glue or similar additives to the build plate to not create unwanted artifacts or a lack of adhesion. For the applications of self-sensing materials PLA seems to be the better choice but in cases that the mechanical or thermal properties of ABS are preferred, then ABS can be used as well.

3.1.4 Conductive Ink

Conductive inks are available COTS in traditional ink cartridges together with a conductive element such as silver particles, carbon nanotubes or carbon black giving the material its piezoresistivity. The conductive elements can also be purchased separately and added to inks. By buying them separately the conductive inks can

be custom fabricated, which is generally done in research literature [39]. The fabrication is not difficult since it only constitutes mixing a conductive filler powder into liquid ink. Conductive inks are often printed through inkjet or DW. Aerosol jet printing with silver-based inks for the purpose of strain sensing has been done as well [70]. They're all methods of dispersing inks, often with many nozzles and capable of creating sheets of material. Conductive inks can experience piezoresistivity making them possible for use as strain gauges [16]. Stereolithography (SLA) or Digital Light Processing (DLP) resin prints can be used to complement the conductive inks as the structural material [15, 39]. The *Diamatix DMP-3000* inkjet printer printing a functional self-sensing part has been demonstrated [39]. The inkjet printer is often more of an industrial grade machine and expensive, it can be bought COTS and includes a feeding mechanism, nozzles and everything needed to create the piezoresistive element. The availability of inkjet printers is lower than both robot arms and traditional FDM printers which is a detriment of the inkjet printer.

3.2 Additive Manufacturing Platforms

The end effector, often consisting of a nozzle, heating element and extruder driver can generally be integrated into many different types of platforms capable of moving the end effector through hardware platform specific G-Code. Different manufacturing platforms have different movement mechanisms, generally showing different strength's and weaknesses in terms of the degrees of freedom, precision, reliability, subpart integration and more. The manufacturing platform and the end effector can be seen as two separate parts of a printer design. The material used and the end effector are very co-dependant, the end effector and the manufacturing platform are not as co-dependant. Some generalizations can be made for different types of end effectors and their compatibility with the manufacturing platform, for example the typical weight for a specific type of end effectors will likely have an impact on the choice of manufacturing platform utilised. Some hardware platforms operate better with a heavy end effector, some hardware platforms provide precision that other's don't, as well as several more performance criteria that can be considered. The additive manufacturing platforms considered will be robotic arms, generic planar FDM 3D printers, inkjet printers, discrete sensor P&P devices.

The spread of the literature from which the review of additive manufacturing platforms is based can be seen in Figure 18.

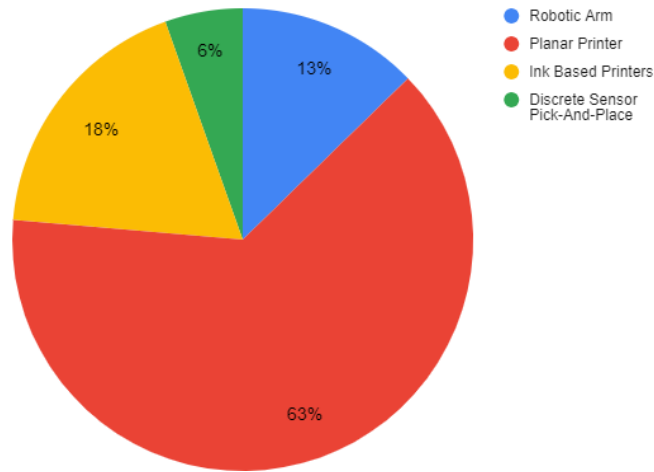


Figure 18: Pie chart of the distribution of papers and patents defining manufacturing platforms that have been included in the literature review.

A majority of literature for the self-sensing materials and continuous CFRTs utilise traditional planar FDM 3D printing. A metric that ties in closely with the additive manufacturing platform as well as the material selection is the type of additive manufacturing method used. A chart showing the literature spread for different printing methods can be seen in Figure 19.

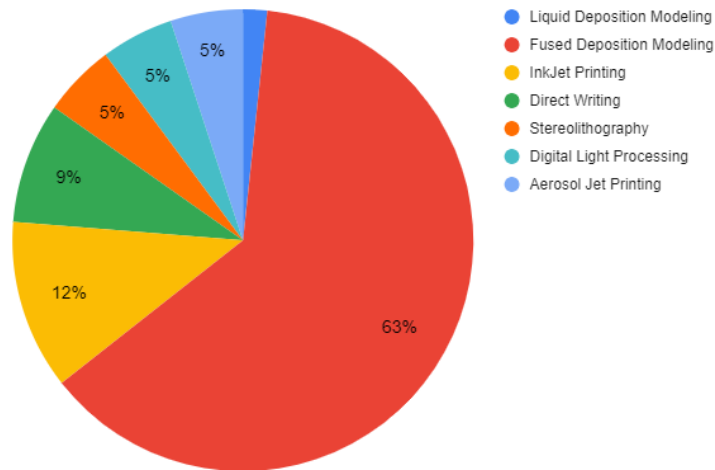


Figure 19: Pie chart of the distribution of papers and patents defining manufacturing methods that have been included in the literature review.

Some sources used designs that were comprised of several different additive manufacturing platforms which in turn used several different additive manufacturing

methods. An example of a multi-material multi-method printer can be seen in Figure 20 [52].

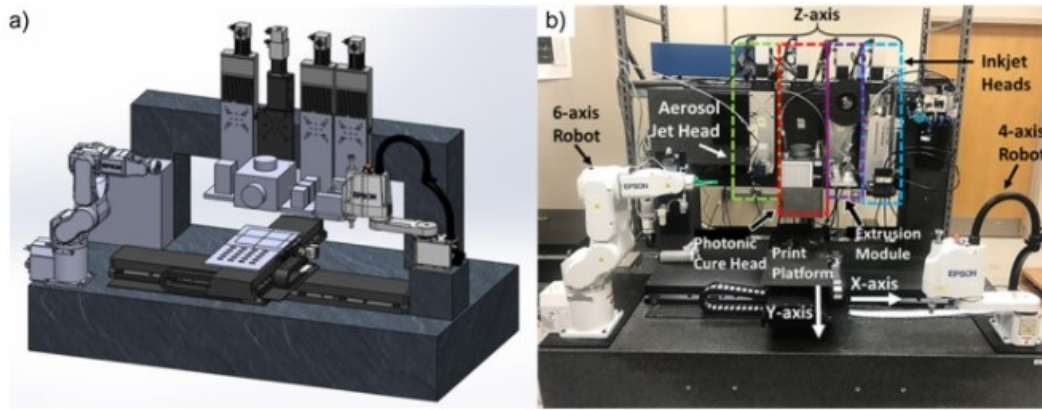


Figure 20: CAD schematic of the m4 hybrid 3D printer. b) A photograph of the assembled printer with each print head, robot, and motion axis labeled [52].

The design used four different additive manufacturing methods which included inkjet printing, FDM printing, DW printing and aerosol jetting. Two robotic arms and a print bed capable of planar and vertical motion made up the movement mechanism for the end effector. On top of all of the various functionalities and technologies used, even photonic curing capabilities were included in the design capable of curing materials. Since the design used several technologies, different parts of the design can be used to justify different design decisions and analysis throughout the literature review and the manufacturability analysis, as well as being included in several categories in the literature spread charts seen in Figure 18 and Figure 19.

3.2.1 Robotic Arms

Utilising a robotic arm as the manufacturing platform comes with benefits such as being capable of the type of motion that traditional planar 3D printers can with the added benefit of six degrees of freedom rather than the three degrees of freedom that a traditional 3D printer would have. Through complementing a robotic arm with a panning and tilting gantry, or other robotic arms even as much as eight, or even twelve degrees of freedom can be reached [29]. Having the nozzle be able to rotate means that printing outside of a flat plane with a change in the nozzle angle is possible. For continuous fibre's this would also mean that the fibre's can be placed in almost any continuous geometry together with supporting material. It may be beneficial for optimizing the sensing properties of the material as well as

the mechanical properties with more omnidirectional placement of fibre's giving self-sensing and structural reinforcing capabilities in any direction in the part. The orientation of CCF's can be highly customized with robotic arms as opposed to traditional planar FDM 3D printing, making the printing of CCF's on curved surfaces such as the example seen in Figure 21 [59] feasible. In general robotic arms can be retro fitted with a 3D printing end effector and the utilisation of continuous CFRTPs through additive manufacturing with a robotic arm has been implemented by several sources of literature successfully [56, 59, 71].

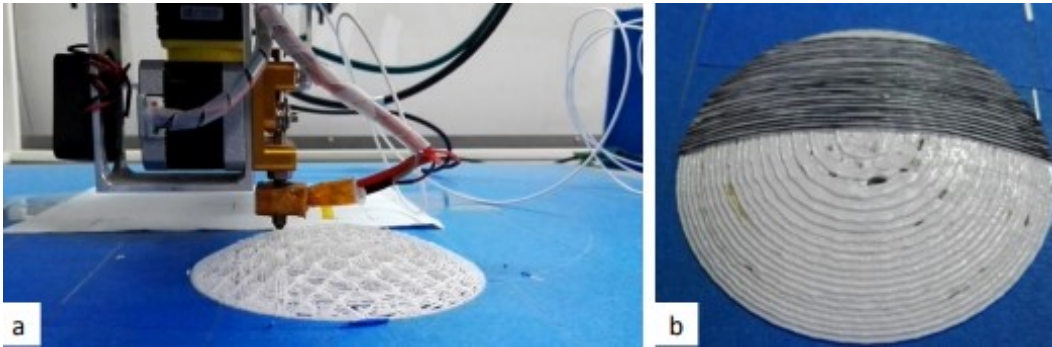


Figure 21: a) 3D printing on a curved surface b) Deposited CFRTPs on a curved surface [59].

Lattice structures can be produced with robot arms, which is where the 3D printed structure can be moved in and out of the plane. It's a form of non-planar 3D printing and an example of lattice printing of continuous fibre reinforced thermoplastics without any supporting material can be seen in Figure 22 [14].

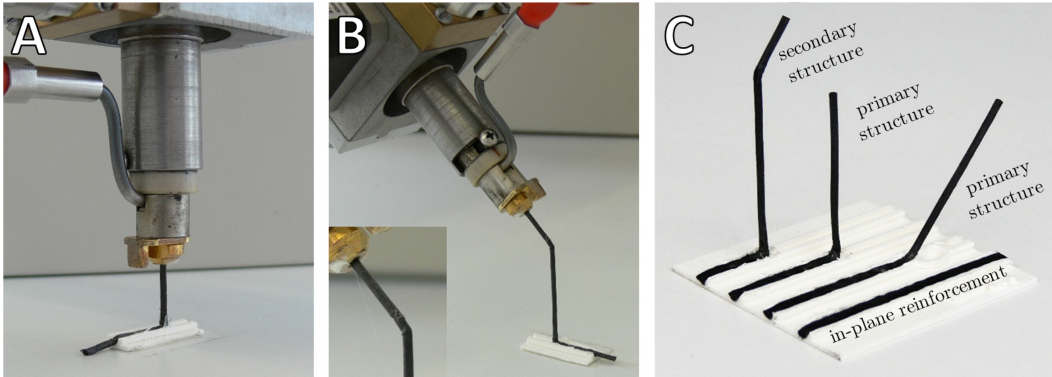


Figure 22: Printing of conductive lithographic film in a lattice structure (A) Primary truss members (B) Secondary truss members. (C) Lattice structure's with different orientations in and out of the plane, one example demonstrates the ability to form secondary structures onto existing members by changing tool paths [14].

The difference in implementing lattice printing for robotic arms as opposed to traditional planar 3D printers is that the nozzle can change the angle of attack with respect to the print surface, which means that the print surface can always be perpendicular to the nozzle direction. Robotic arms can be utilised in conjunction with a traditional 3D printer where software communication between the robotic arm and the 3D printer communicates their relative positions and current operations, taking advantage of the strengths of either method. Traditional 3D printers have very rigid rails to ensure print precision, but a robot arm could be more prone to flexion during printing. Significant flexion while 3D printing is likely to cause print failure. Utilising a method of 3D printing followed by pausing the print and initiating a robotic arm movement is a versatile printing method that has also been used [4]. However a large detriment of using robot arms is the software integration and the technological readiness level when applied in additive manufacturing. The extruder driver and movement of the robot arm needs to be compatible or be made compatible. The robot arm can be made to comply with the G-Code needed for manufacturing any part that could be done with a traditional FDM 3D printer. The software can generally not be a generic 3D printer slicer software due to requiring the operation of more than three motors in the G-Code. There is a up-and-coming robot arm to 3D printer software called Adaxis, who's only mention in literature is the failure modes of additively manufactured composites [2]. In the article an explanation of how Adaxis was used to benefit the research was not provided. Even with the technological readiness being sufficient, software integration will still be more difficult than the software for a traditional planar 3D printer due to robotic arms having various dimensions. Often several software's are run in tandem to op-

erate a robotic arm for the purposes of additive manufacturing [52, 6]. Therefore compared to traditional FDM 3D printers robot arms are more expensive and more time consuming to implement.

3.2.2 Planar Printers

Traditional planar FDM 3D printers have full freedom of motion in the plane and build the part by incrementing just the vertical coordinate between layers. Having simple planar motion together with either the nozzle or the build plate move to create the distance between the print layers means relatively few motors with very predictable motion. The printer is supplied with a 3D printing end effector and is the most utilised printing method for the additive manufacturing of self-sensing materials which can be seen in Figure 18. A bowden Polytetrafluoreten (PTFE) tube is generally used to feed the material from the filament spool to the nozzle, but direct drive systems can in some cases be more reliable where the extruder driver is fit onto the end effector. The extrusion speed is determined through extrusion values in G-Code whilst the movement motors move the end effector in three degrees of freedom. A driver board consisting of relays for the motor but also the memory and interface of the printer can generally be bought separate if improved driving of the motor's is preferred or more motors are needed. Having the main board be relatively interchangeable is a strength for utilising a COTS traditional planar 3D printer.

The planar printing hardware platform has been used for producing parts from pre-impregnated continuous fibre's for non self-sensing applications with COTS printers such as the *Mark Two* and *X7* by *Markforged* [69, 53]. More affordable 3D printers such as the *Prusa i3* by *Prusa* used as a base where the end effector is modified to be capable of CCF extrusion shows that modified general purpose 3D printers are viable for the printing of CCF [13]. SLA printing is also a form of planar printing but can only be utilised for the structural part of the material due to printing with resin [39]. SLA printing on It's has not found to be able to manufacture piezoresistive materials in literature, and will therefore not be considered for the fabrication of self-sensing materials. Custom printing systems either for CCF or thermoplastics generally utilise planar printing [38, 16, 62]. Although 3D printers are designed for planar printing the printers are not constrained to it. Movement in both the plane and the vertical axis is possible with traditional planar FDM 3D printers, a process that is called non-planar 3D printing [55, 1]. Non-planar 3D printing is often constrained to shallow angles due to the nozzle or fan case being in the way. Robot arms and rotating bed gantries for the non-planar 3D printing don't have this issue due to the nozzle being directed at the print surface at all times. A

figure illustrating the end effector geometries limiting the print due to either nozzle or fan case obstruction are visualized in Figure 23.

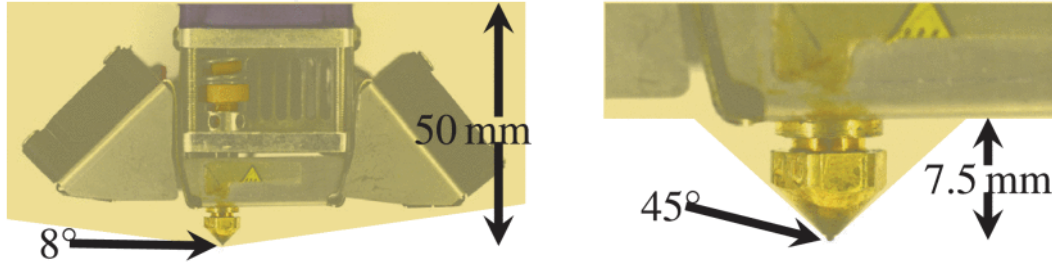


Figure 23: The collision model of the *Ultimaker 2* 3D printer. The left image is taking the whole printhead into account where $\theta_{np}=8$ and non-planar height is 50 mm. The right image is only taking the nozzle into account with a $\theta_{np}=450$ and a non-planar height of 7.5 mm. With these configurations, either large surfaces with a small θ_{np} or small surfaces with a large θ_{np} can be printed [1].

Examples of non-planar lattice printing with continuous carbon reinforced thermoplastics has also been shown to be possible, with varied success. Euler buckling and fibre debonding are prominent issues of the planar additive manufacturing of CCF reinforced plastic lattice structures [63]. An example of utilising lattice printing with a planar 3D printer along with the resulting printing characteristics of a truss can be seen in Figure 24.

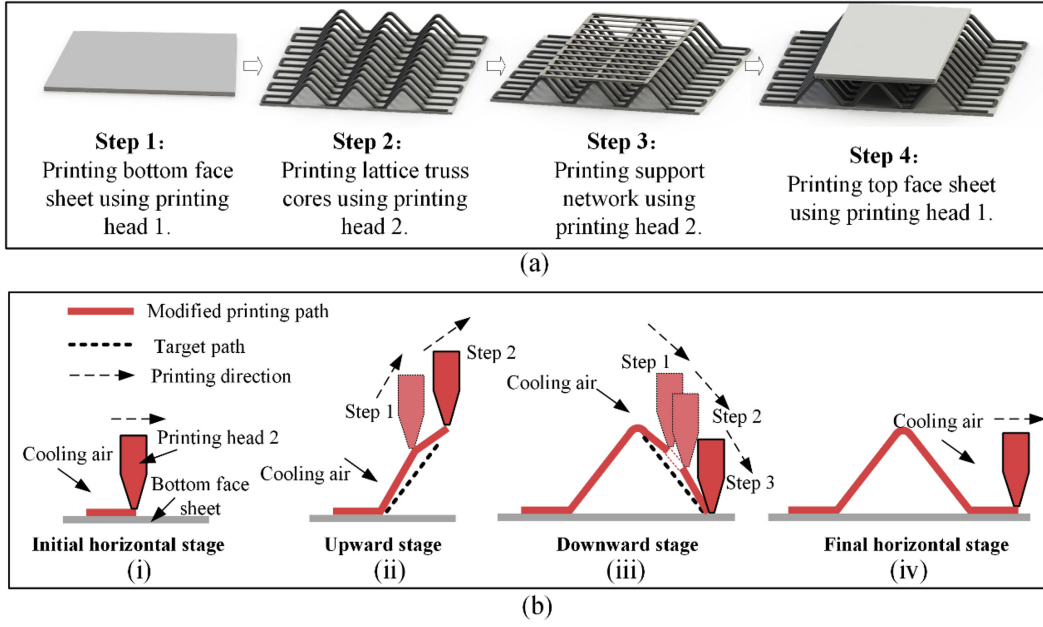


Figure 24: (a) Illustration of fabrication approach 3D printing lattice structure's. (b) Schematic of printing triangle truss core processes [63].

Having a 3D printer be capable of non-planar 3D printing can improve the mechanical properties of the material as well, non-planar 3D printing of three dimensional strands as the upper layer of a CCF structure has been suggested to improve the mechanical properties of the 3D printed part in the vertical direction [50, 1]. Improved surface finish can also be achieved with non-planar 3D printing, which on It's own has shown to give improved mechanical properties for additive manufacturing [36]. Having the fibre support the thermoplastic matrix in complex geometries such as cellular structures can both reduce the weight of the part as well as provide improved mechanical properties and resistance to omnidirectional stress. An illustration of a cellular 3D printed structure can be seen in Figure 25.

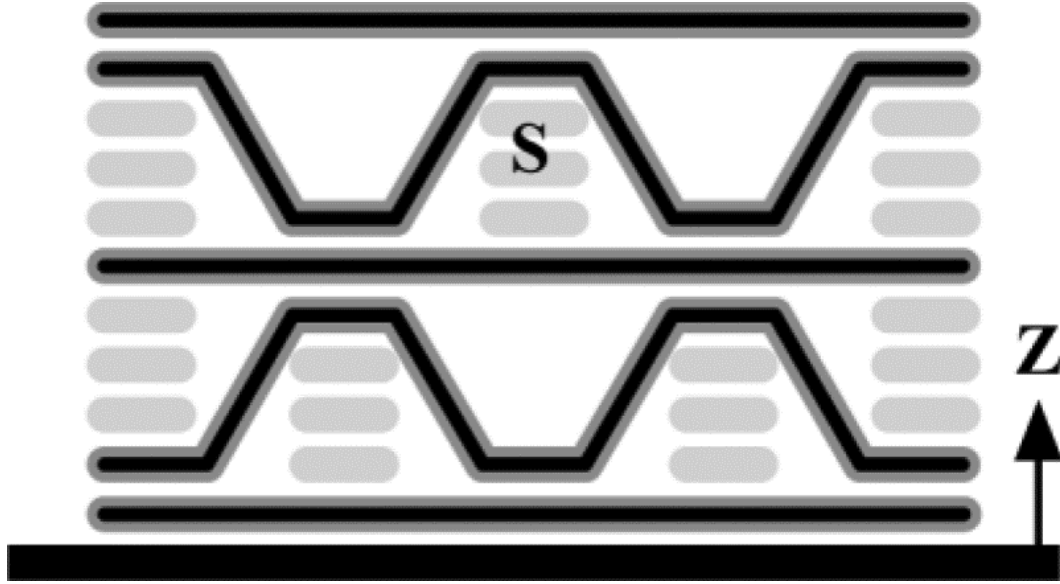


Figure 25: Cellular 3D printed structures with the black lines representing the strands of CCF [50].

The structural thermoplastic matrix can be seen under the CCF's. The carbon fibre aims to give the material improved mechanical strength but may also alter the self-sensing properties of the material due to introducing both bending and tensile forces in one strand of continuous fibre. A three dimensional sensor could be conceptualized with the use of cellular structure's. Additively manufactured self-sensing properties of cellular CCF structure's has not been tested in literature.

A strength in the utilisation of planar 3D printers is the large set of available information and a widespread retrofitting community such as the RepRap platform commended by It's availability of educational content [28]. Open source repositories with a lot of functional scripts and software are widely available and often compatible with FDM 3D printers. A factor contributing to that is that the G-Code used by the 3D printers use highly standardized commands and formatting. The flavor of G-Code is a term that describes how a 3D printer interprets the geometrical commands is highly standardized and documented. Open source non-planar 3D printing scripts and software can convert G-Code to operate the vertical movement motor throughout the tool path. It allows for the sensing materials or the structural material to be set at an angle, yielding both sensing accuracy in different directions but also opening up the possibility of more omnidirectional mechanical properties. The omnidirectional mechanical properties would have the greatest affect when paired with a highly anisotropic material such as CCF's and varying their direction.

3.2.3 5-Axis Printer

utilising a COTS planar 3D printer with a rotating gantry providing print bed rotation is called 5-axis printing, or 5d printing, since it operates in five dimensions rather than the three dimensions of movement that the planar printer is constrained to. It is however one degree of rotational freedom less than available for a robotic arm. The method does however see many of the advantages of robotic arms as the platform for additive manufacturing, while lowering the entry barrier for accessing those advantages. A 5-axis printer utilising a *Prusa i3* by *Prusa* as the 3D printer and a custom rotating gantry for the print bed resulting in a 5-axis printer can be seen in Figure 26 [24].

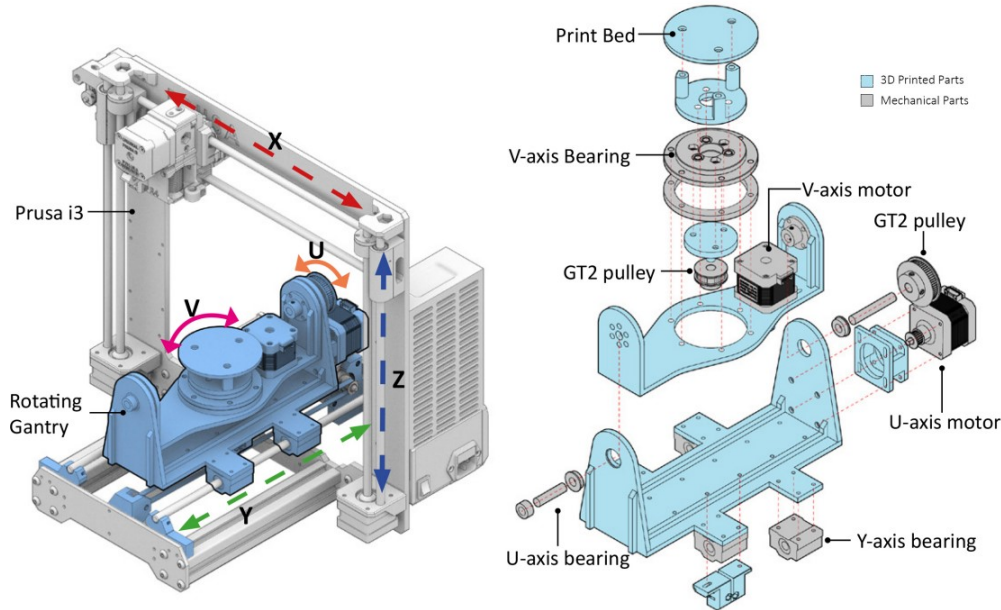


Figure 26: The left image shows the arrangement of the 5-axis 3D printer with the 2-axis mechanism built-into the existing *Prusa i3 MK3s*. The 2-axis rotary gantry is indicated in blue and the 5 axes (X,Y,Z,U & V) are illustrated with colored arrows. The right image shows an isometric drawing of the 2-axis rotary gantry. The 3D printed parts are cyan and the commercial parts are grey [24].

The traditional printing axes (X, Y, Z) are provided by the COTS *Prusa* 3D printer but the print bed rotation supplies the 3D printer with two rotational axes (U, V). The rotation axes make the 5-axis printer end effector positioning with relation to the printed part more versatile compared to a traditional 3D printer. The material

and specifications are mostly open source, but are going through a transition period where 5-axis printing still has limitations in software, design specifications and COTS availability. The capability of printing conductive PLA has been shown with a 5-axis printer [24]. The printing of continuous CFRTP utilising PLA as thermoplastic at a fibre fraction of 16 % has also been done in 2022 [67]. The configuration utilised a dual nozzle extruder and the additive manufacturing configuration can be seen in Figure 27.

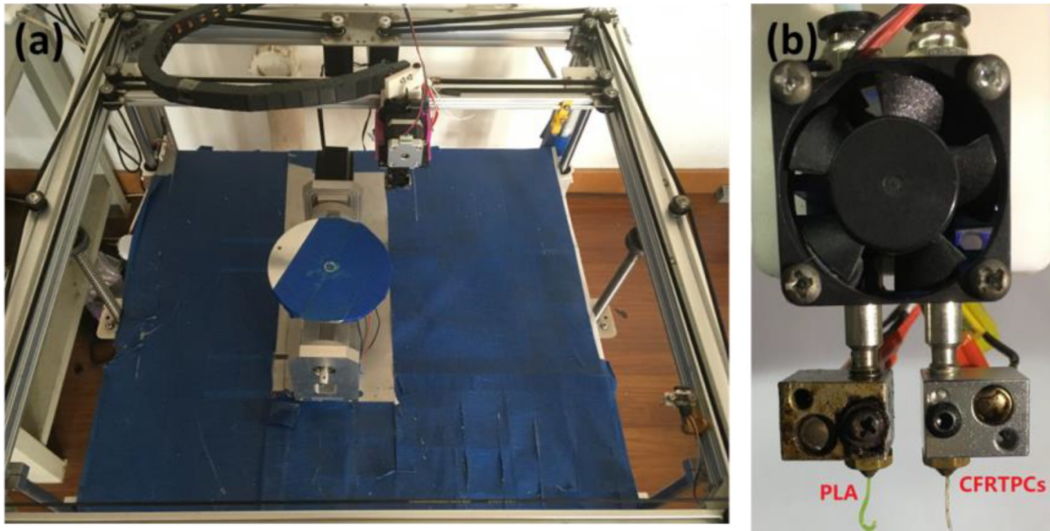


Figure 27: (a) The experimental 5-axis platform. (b) The dual extrusion end effector [67].

A 5-axis printer can give the material strain sensing capabilities in any direction by altering the orientation of the part throughout the print. Measuring the strain in different directions can also provide omnidirectional mechanical properties, especially when utilising CCF's or another strong material as the sensor. Not all content for producing the 5-axis printer is open source, which for now makes the implementation of a 5-axis printer harder. The hardware for the rotating bed gantry is custom and can not be found as any sort of COTS product. Relatively good hardware specifications are available, making the implementation of a 5-axis 3D printer possible [22]. Having a reliable traditional planar 3D printer with high levels of printing precision and reliability as the base, together with printing at most angles with respect to the part can result in very reliable parts and sensor structure's without using a robotic arm.

3.2.4 Ink Based Printers

Inkjet, aerosol jet, & DW printers can print additively manufactured strain gauges with piezoresistive inks [39]. Droplets of material get deposited onto a build plate which creates a thin layer of material and depending on its piezoresistive characteristics it can be used as a strain gauge as well [5, 16]. The printers are tailored towards industry and COTS markets are limited for inkjet or DW printers. Ink based printers are limited by their capability of only printing ink based parts. While the piezoresistivity of conductive inks are proven, integrating them into a load bearing structural part is more difficult [39]. Ink based printers such as inkjet printers are generally used for scientific purposes or for making circuitry rather than as structural parts. This means that the printer likely has to be combined with a different type of printer as well which then is capable of printing a structural part. Having ink based printers print outside the plane is also not possible, which is another detriment of using both ink based printers.

3.2.5 Discrete Sensor P&P Machine

A discrete sensor P&P machine can be utilised in conjunction with a 3D printer in order to place sensors or other structures into a structural 3D printed part during printing. Software integration between the discrete sensor P&P machine and the 3D printer is required [7, 15]. A system utilising both a pneumatic P&P system together with a FDM printing method can be seen in Figure 28 [15].

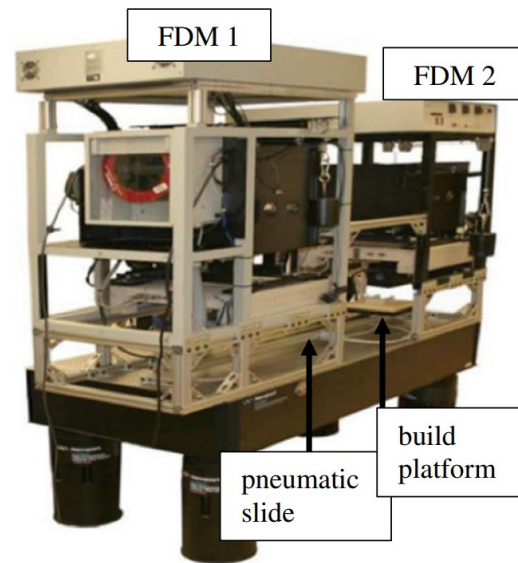


Figure 28: The multi3D system using two FDM platforms together with a pneumatic system [15].

Discrete sensor P&P machine's are more applicable for non-filament type sensors which is why It's being considered together with discrete sensors. If the sensor were to be filament based it would generally be easier to extrude it rather than place it. But if high sensing accuracy is required, as well as where the structural rigidity is not a large focus then a P&P system together with a planar FDM 3D printing system could be utilised. The sensors, likely being Microelectromechanical Systems (MEMS) based sensor's would mean placing a large gap in the material, which can create weak points in the material affecting It's load bearing capability and homogeneity. Since the wiring of the sensor is not the self-sensing material itself the wiring would need to be made between the sensor and the measurement points. The wiring would most likely have to be placed manually defeating part of the purpose of additively manufacturing the part. Sensing precision would likely be much higher than other alternatives due to discrete MEMS sensors being designed for sensing with very tight tolerances. The pneumatic device could place other components electrical or otherwise into the material as well.

3.2.6 Nozzle

A nozzle is used for where the configuration of the additive manufacturing process includes an FDM end effector. There are abrasive materials with a high tensile modulus such as carbon fibre based materials that wear down commonly used brass

nozzles, hence more abrasion resistant nozzles can be required [20]. An example of what damage the extrusion of abrasive materials can do to a nozzle can be seen in Figure 29. A nozzle for printing carbon fibre parts can be a steel nozzle [57].

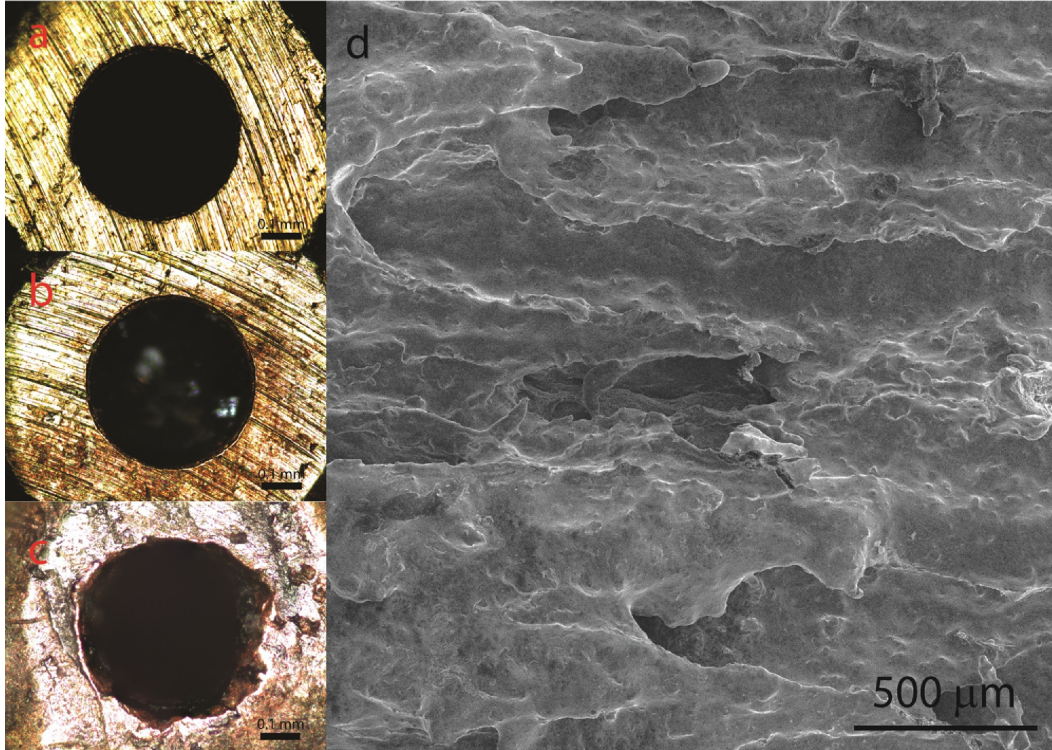


Figure 29: Optical micrographs showing the surface of a 3D printing nozzle before and after printing. (a) Unused nozzle. (b) Nozzle after printing 10 cm of PBT/graphene. (c) Nozzle after printing 1.5 m of PBT/carbon nanotube. (d) Scanning electron microscope image of PBT/graphene composite printed with an abraded nozzle [20].

Dual extruder configurations require two nozzles, one for printing the sensor and one for the structural thermoplastic matrix. The nozzle size and hardness can be tailored towards what that specific nozzle is printing. When utilising for example carbon nanotubes as the sensor in a polymer matrix a separate nozzle and extrusion point can be utilised for either material [32, 33]. Co-extruding nozzles have a single extrusion point with more than one entry point which is used for printing multiple materials with overlapping printing temperatures and a mix of the materials in the nozzle can function similarly to what a dual extruder configuration does [20]. In the case of continuous fibre's, PTFE tubing can be inserted into the nozzle to minimize

the risk of fibre snagging as well [13].

When using PTFE tubing as a filament guide, the toxicity of PTFE at high temperature's need to be taken into account. PTFE tubing close to the nozzle at a high thermal load can produce micro particles which cause pulmonary affects in humans and especially animals [30, 58]. The print bed material for any CFRTP needs to have a high level of adhesion and to be heated due to the difficulty of printing the material. A garoline print bed coated with Polyvinyl Alcohol (PVA) solution has been utilised for the printing of continuous CFRTPs [13]. PP-plate has been utilised for the printing of short CFRTPs which are also difficult to adhere to a build plate [57].

3.3 Software

Various types of slicing software's can be used to generate the G-Code, movement speeds, direction, extrusion speeds, nozzle temperature, bed temperature, filament retractions and much more get determined through the slicer software. There are slicing software's that are open-source, and able to customize the G-Code such as the *FullControl* G-Code designer [19]. Another software utilised for intricate G-Code manipulation is *Fabrix* [35] which is a highly customizable G-Code generation software. *Slic3r* is often used in literature when the slicing does not have to be as customized [4, 40]. For G-Code manipulation *Repetier-Host* has been used for modifying printers to be capable of CCF printing after a slicer software has generated the base G-Code [66, 40, 38].

The design will likely implement motor start/stop commands for the sensor extrusion, implement cut commands if CCF was used and has to be cut, and likely adding safety delays for the commands that pause the G-Code. Due to those reasons the level of G-Code manipulation possible has to be a focus in the software used. Something most relevant for the additive manufacturing of CCF [40] due to the inclusion of a cutter. Software's such as Eiger provided by the *Markforged* company for their 3D printers is very closed-off and is limited by where fibre can be placed. The Eiger software has CCF placement commands and functionality integrated into the slicer and the printers are often used for printing of fibre reinforced polymers [61, 59, 13, 71, 53, 68]. Placing contact points is not feasible with Eiger and having non-planar movement is not possible.

Software companies making robotic arm FDM 3D printing easier to integrate exist, but the industry is not as developed as that for traditional planar FDM 3D printers. A more generalized robotic arm FDM 3D printing system has been developed by

the company Adaxis [2].

3.4 Literature Review Conclusion

The most prominent methods for the additive manufacturing of self-sensing materials leaned towards a FDM printing method with planar printers using CCF's at the piezoresistive element in the self-sensing material. Having the CCF not only be capable of acting as the piezoresistive element but also as a structural part is in the favor of using it as the sensor. Ink type printers and conductive inks are capable of reliably producing the sensor, but do not produce the structural part, which is a limiting factor for using ink as the sensor in the self-sensing material. Conductive thermoplastics are easily usable but do not provide any additional structural rigidity to the part. Carbon nanotube doped thermoplastics are feasible to use as the piezoresistive element but are not available COTS. Having more degrees of freedom is seen as a beneficial factor but is not as common as a traditional planar FDM 3D printer. Software's required highly depend on the application, platform and material. More degrees of freedom require more niche and less available software, which again speaks to the use of traditional planar FDM 3D printers. The introduction of non-planarity to the printer can however improve the design freedom. An area of lacking literature is the data interpretation of additively manufactured three dimensional sensor structure's in the material, such as cellular structures. Knowing what strain data a three dimensional sensor can provide and if there are real world benefit of that data can further justify the implementation of cellular structure's or other three dimensional sensor layouts.

4 Manufacturability Analysis

The manufacturability analysis will determine the feasibility of implementing self-sensing materials with the hardware configuration available, which is a planar FDM 3D printer, the *Crealty Ender 3*, PLA thermoplastic as well as two configurations of CCF tow, 3K and 12K tow. The hardware availability means that ink based printing and discrete sensor P&P devices can not be analyzed in a real world setting within the scope of the work. Different manufacturing methods based of the literature review and material properties for self-sensing materials has provided an insight into the implementation feasibility of various materials. The capability of extruding filaments that have been post-processed into a 3D printer compatible format will be considered possible to print, especially COTS 3D printing filaments such as ProtoPasta and Carbomorph. Carbon nanotube filaments with unspecified carbon nanotube wt% exist which makes their level of piezoresistivity undefined, as well them being categorized under printing filaments. Manufacturing carbon nanotube based filaments require filament fabrication hardware not available.

Dry CCF is available and is printable with a modified planar FDM 3D printer which can test the feasibility of implementing a design. Lab results and personal experience using the hardware available together with the base of data from the literature review will be used to govern the testing procedures and sought after result of the analysis.

Testing and proving the manufacturability of geometries and a design that's not feasible on existing CCF printers in literature or in industry was a focus. Dry CCF's integrated into a non-planar 3D printed part printed with a COTS FDM 3D printer for self-sensing could not be done through existing hardware such as the *Markforged* 3D printer due to software constraining the sensor structure geometries. Another reason is that the *Markforged* printers use pre-impregnated CCF filament which through lab measurements against dry fibre has shown a much greater resistance at the measurement points. The strength of utilising a pre-impregnated fibre would be higher rigidity of the filament before printing which means that the extrusion of it is easier which may improve the reliability of the material extrusion. Literature has seen the implementation of CCF's in lattice 3D printed structures. But non-lattice 3D printed dry carbon fibre's for self-sensing has not been done. The capabilities to optimize non-planar G-Code for CCF printing will be validated as well.

The printing of the electrical contacts outside the structure is feasible through a custom design, which is highly preferred in order to not compromise the material

after the printing has already been done. The alternative is inserting metal wires into the part, which is feasible and can generate a reliable electrical contact but it means melting wires into the material which could compromise the structure of it. The adhesion between the wire and the continuous fibre can not be inspected and the reliability of the connection can not be quantified. For cases where denser or more complex sensor structure's are used, the manual insertion of wires could be deemed infeasible due to the lack of precision. An example of a part with metal wire connections has been produced in the lab, and can be seen in Figure 30.

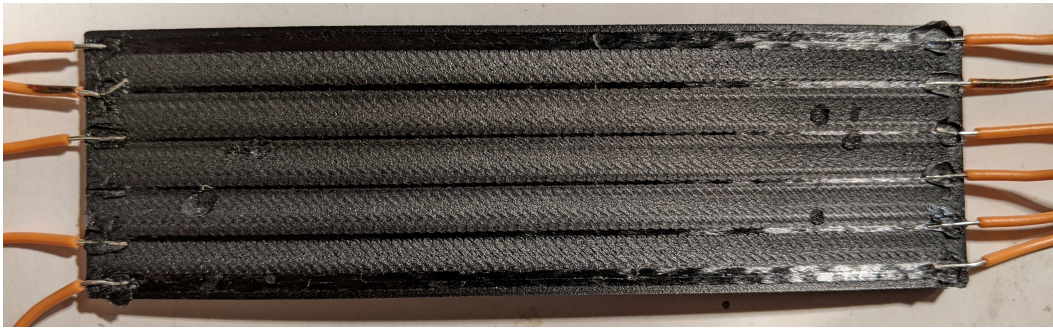


Figure 30: Nylon sheet with embedded CCF's printed with the *Markforged X7* industrial 3D printer. Metal wires are interfaced with the CCF's through melting the wire's into the material where predetermined spots for fibre interfaces have been placed.

Contacts integrated through printing of the CCF's can be seen in the matrix of connection points in Figure 13, which is a highly preferred design due to having less opportunities for human error, as well as not affecting and possibly compromising the structure of the part. The printing path needs to be altered and additional G-Code lines need to be implemented for the laying of the contact points. A purge tower, which is a structure on the 3D printing bed where an amount of material gets dispersed for non-functional use could be utilised to straighten out the CCF's for the next lay up of fibre's. For the extrusion of CCF's a direct drive extruder should be utilised, especially for dry fibre. A direct drive extruder will give the fibre's less opportunities to buckle for when a cut in the fibre is done.

4.1 Filament Test

The purpose of the filament tests is to ensure the adhesion between the sensor and the thermoplastic PLA matrix, as well as verifying an electrical connection of the fibre through the PLA. By first generating a test piece in SolidWorks, for which the

blueprints can be seen in Appendix A a 70 x 4 x 2.8 mm model was designed. The dimensions were chosen so that 11 layer's are printed when slicing at a layer height of 0.2 mm. For the test a 0.4 mm nozzle was used. Overhangs for where the fibre should be placed were generated in the model. The low amount of layers means that the model can be printed quickly but also makes the later G-Code manipulation easier. There will be significantly less lines of G-Code to scroll through and edit. The file was exported to an STL file format compatible with slicer software's. Through the *Ultimaker Cura 4.11.0* slicer the initial G-Code was generated. The start G-Code for the *Ender 3*, which uses the Marlin flavor can be seen in Listing 1. The end of *Ender 3* G-Code can be seen in Listing 2.

Listing 1: *Ender 3* start G-Code.

```
G92 E0 ;Reset Extruder
G1 Z2.0 F3000 ;Move Z Axis up
G1 X10.1 Y20 Z0.28 F5000.0 ;Move to start position
G1 X10.1 Y200.0 Z0.28 F1500.0 E15 ;Draw the first line
G1 X10.4 Y200.0 Z0.28 F5000.0 ;Move to side a little
G1 X10.4 Y20 Z0.28 F1500.0 E30 ;Draw the second line
G92 E0 ;Reset Extruder
G1 Z2.0 F3000 ;Move Z Axis up
```

Listing 2: *Ender 3* end G-Code.

```
G91 ;Relative positionning
G1 E-2 F2700 ;Retract a bit
G1 E-2 Z0.2 F2400 ;Retract and raise Z
G1 X5 Y5 F3000 ;Wipe out
G1 Z10 ;Raise Z more
G90 ;Absolute positionning

G1 X0 Y0 ;Present print
M106 S0 ;Turn-off fan
M104 S0 ;Turn-off hotend
M140 S0 ;Turn-off bed

M84 X Y E ;Disable all steppers but Z
```

The code shows what settings were used for the print. Furthermore some G-Code manipulation had to be done for the file. A stop command was generated right before transitioning into the 6th layer, where the CCF's are to be placed. Inserting the pause in the G-Code rather than pausing the print through the printer's display

interface means that the pause will happen at the exact line of code chosen. The pause command, together with moving to an idle position as well as the code that is run when the print is resumed can be seen in Listing 3.

Listing 3: *Ender 3* pause G-Code.

```
;TYPE:CUSTOM
;added code by post processing
;script: PauseAtHeight.py
;current layer: 5
; switch to relative E values for any needed retraction
M83
G1 F300 Z2.4 ; move up a millimeter
G1 F9000 X190 Y190
G1 F300 Z15 ; too close to bed--move to at least 15mm
M104 S0 ; standby temperature
M0 ; Do the actual pause
M109 S200 ; resume temperature
G1 F300 Z1.4
G1 F9000 X94.3 Y117.7
G1 F300 Z1.4 ; move back down to resume height
G1 F2700 ; restore extrusion feedrate
M82 ; switch back to absolute E values
G92 E115.93119 ;<- 120.93119 - (101.90107 - 96.90107)
```

The pause command gives a prompt on the user interface of the 3D printer to press the start button once more to resume the print. The *G92* command restores the flow rate which is calculated by taking the sought after flow rate in the first line of the next layer and removing the difference of the previous non-altered flow rates from the value. Other G-Code manipulation that's included is altering the flow rates to account for the added CCF generating a more optimized tool path for the layer where the CCF should be placed. The G-Code is categorized into different sections, outer wall, inner wall and infill. The first alteration is to move the outer wall printing ahead of the inner wall printing in the G-Code. By doing this the outer wall will be printed first and a straight line across the part can be made at a lower flow rate which adheres the fibres to the PLA thermoplastic matrix. Within the outer wall G-Code the lines seen in Listing 4 were changed with the G-Code manipulation mentioned resulting in the G-Code seen in Figure 5.

Listing 4: 6th layer wall G-Code.

```
G1 F1200 X82.7 Y117.55 E118.00962
```



```

G1 X82.7 Y117.45 E118.01361
G1 X92.7 Y117.45 E118.41273
G1 X92.7 Y115.7 E118.48258
G1 X142.3 Y115.7 E120.46222
G1 X142.3 Y117.45 E120.53207
G1 X152.3 Y117.45 E120.93119
G1 X152.3 Y117.55 E120.93518
G1 X142.3 Y117.55 E121.3343
G1 X142.3 Y119.3 E121.40415
G1 X92.7 Y119.3 E123.38379
G1 X92.7 Y117.55 E123.45364
G0 F9000 X93.14 Y117.239
G0 X93.3 Y117.239
G1 F2700 E118.45364

```

Listing 5: Altered 6th layer wall G-Code.

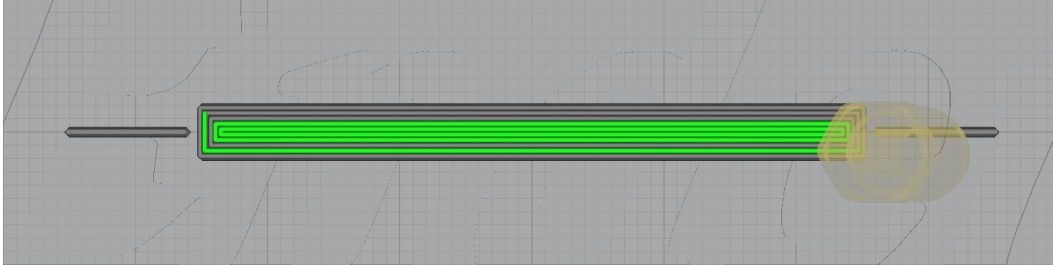
```

G0 F1200 X82.7 Y117.55
; Print Line Across
G0 X82.7 Y117.45
G1 X152.3 Y117.45 E120.93119
; CCF placed
; Move Left
G0 F1200 X142.3 Y117.45
G1 X142.3 Y119.3 E121.40415
G1 X92.7 Y119.3 E123.38379
; E(123.38379+121.40415-120.93119)
G1 X92.7 Y117.45 E123.85675
; Move Right
G0 F1200 X142.3 Y117.45
; E(123.85675+121.40415-120.93119)
G1 X142.3 Y115.7 E124.32971
; E(123.82971+123.38379-121.40415)
G1 X92.7 Y115.7 E126.80935
; E(126.40935+121.40415-120.93119)
G1 X92.7 Y117.55 E127.38231
G0 F9000 X93.14 Y117.239

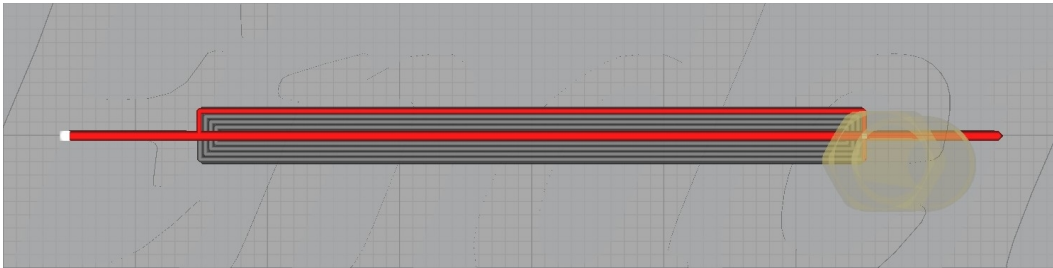
```

The comments on several of the lines were used to calculate what the next extrusion value should be for the amount of movement. The accumulative flow is the number after the letter *E*. Due to changing the order of the lines of code the same amount

of flow between positions had to be kept for the same amount of movement for a consistent flow rate. On layer 5 the first unaltered filament placement path can be seen in Figure 31a and the altered path can be seen in Figure 31b.



(a) The 12 first G-Code commands finished on layer 5 on the unaltered version of the test piece.



(b) The 7 first G-Code commands finished on layer 5 on the altered version of the test piece.

Figure 31: *Ultimaker Cura* slicer interpretation of the G-Code for the model.

The accumulative type of extrusion where the difference between the extrusion value between lines of code determines the amount of material to be dispersed is called absolute extrusion and is the nominal and recommended extrusion method for the *Creality Ender 3*. Since the absolute extrusion example could produce a part, a relative extrusion part has also been printed which has shown the same level of success. Relative extrusion is when the amount of material to be dispersed between the length of movement is defined in the G-Code as the extrusion value, rather than the difference in extrusion values. Less hand calculations have to be made due to not having to work with accumulative values. Some 3D printers are not compatible with relative extrusion values and It's not the recommended setting in *Ultimaker Cura 4.11.0*, but with the current hardware it still works. Relative extrusion is enabled through the command *M83* in the start G-Code.

Filament will be integrated into the to test the CCF and PLA adhesion as well as the capability for the printer to print over the CCF. Having the change in G-Code

for the extrusion path allows fibre's to be placed on a modified path. The filament will be integrated into the material when the stop command is issued, and for further adhesion a glue stick was used to keep the fibre in place when being printed over. The specific CCF tow used was a 3K filament by Easy Composites split into two resulting in a roughly 1.5K filament [8]. A 6.5 cm piece of dry CCF was laid down onto the part, leaving connection points large enough to reliably measure the resistance through the part on either end. In Figure 32 the print is paused at the pre-determined layer height through the the G-Code in Listing 3. The CCF's were placed in the middle of the part with fibre's protruding from both ends where electrical measurements can be done for validating the connection through the part.

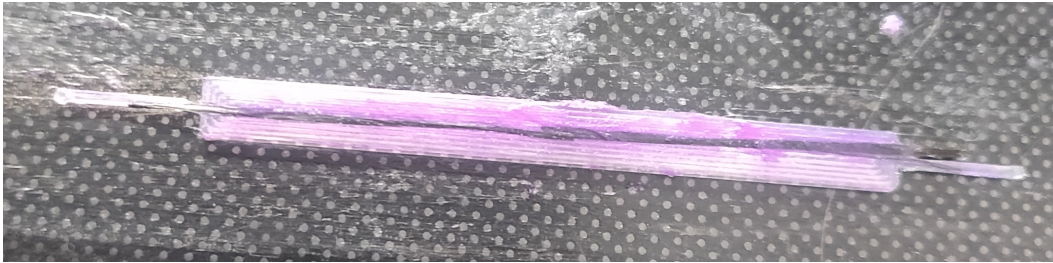


Figure 32: The internal structure of the CCF's.

Lay up of CCF's mid-print only validates parts of the manufacturing method. For the actual additive manufacturing of functional self-sensing parts, there should not be an interruption in the printing process. Laying the CCF's while also disrupting the layer height at that spot could significantly affect the reliability of the additive manufacturing process and part. Software can take into account the height of the CCF's but a manual lay up of the fibre can not be as precise as a 3D printer. Having the fibre's be additively manufactured comes with its own issues such as fibre buckling and possibilities of nozzle clogging or the fibre getting stuck somewhere along the feed line. Having dry fibre extruded through the same nozzle as a polymer may be beneficial as the fibre can cure in the nozzle which can improve the mechanical properties of the fibre and the 3D printed part.

Once the print was completed and the carbon fibre's were joined in the middle of the PLA part, electrical measurements could be made on the part. The electrical conductivity test showed a reliable and relatively low resistance connection between the fibre. Results of the electrical measurements can be seen in Figure 33 where a $340\ \Omega$ resistance was measured. Depending on how many of the fibre's could be connected to the multimeter the resistance could get down to $180\ \Omega$ if pressed firmly against the probes.



Figure 33: Test bench for measuring the resistance of the CCF in the PLA thermo-plastic matrix.

The printed part showed that bonding between COTS PLA printed with a COTS *Ender 3* 3D printer to the dry CCF is possible, which makes its printability feasible as long as the extrusion of CCF's can be done as well. The result was successful.

4.2 Extrusion Tests

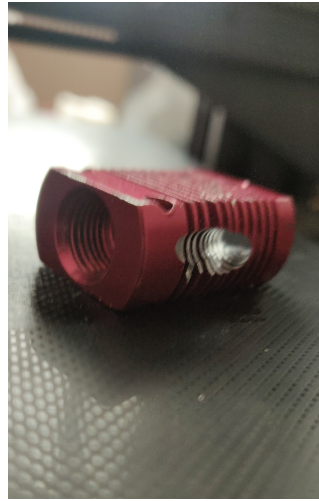
Extrusion tests where both PLA and CCF's get extruded through the same nozzle at the same time were achieved. To get more space for both the thermoplastic filament and the CCF to make it out of the nozzle, a nozzle with a diameter of 1 mm was used. The nozzle size chosen is significantly larger than the included 3D printing nozzle of 0.4 mm, which is a very typical nozzle size. Having a larger nozzle means that CCF's with higher filament counts with a larger combined diameter can be extruded. Due to the high level of abrasion of the CCF on metals such as brass which is the typical nozzle used for 3D printing, a steel nozzle was used instead.

The feeding of the CCF was done through drilling into the radiator and the heat break allowing PTFE tubing with a diameter of 3.95 mm to be inserted into the drill hole making contact with the existing bowden tube used to feed thermoplastic filament into the nozzle. The CCF's get joined where the PLA is semi-solid. If the PLA was to be too melted where the hole was made, back pressure could build up and thermoplastic could start moving into the CCF feeding point. It could clog the CCF's and possibly also the thermoplastic. If the thermoplastic were to be com-

pletely solid, the CCF's would have a difficult time getting moved into the nozzle since there would be a lack of grip between the thermoplastic and the fibre. Drilling into a point where the thermoplastic is expected to be semi-solid is expected to be the most reliable way of extruding CCF's and thermoplastic through the same nozzle. The drilling was done with a drill press using a hardened steel drill bit and metal lubricant. The initial drill bit had a diameter of 2.5 mm, where after a drill bit of 4 mm was used giving the final dimension for the drill hole. Since the edges of the radiator and heat break were very sharp and rough some filing of the edges was done after. The heat break with a drill hole can be seen in Figure 34a, and the radiator with the drill hole can be seen in Figure 34b. The radiator is installed on the heat break to complete the structure, which can be seen in Figure 34c.



(a) Drill hole in the heat break while attached to the heating block.



(b) Drill hole in the radiator.



(c) The radiator and heat break combined with the drill hole's aligned.

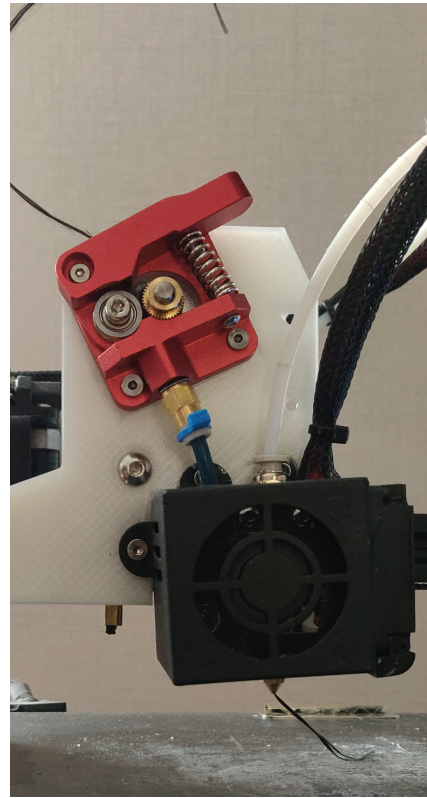
Figure 34: Drill holes in the *Ender 3* 3D printer to allow CCF's to be extruded through the nozzle together with thermoplastic.

The PTFE bowden tubing for the PLA could now be inserted into the heat break with the side of it exposed through the new drill hole. Where the PTFE tube is exposed through the drill hole a cut needs to be made to allow access to the filament inside the tube. Due to the PTFE tubing having fairly small tolerances to the 1.75 mm PLA filament the inside portion of the tube from the drill hole to the nozzle needed to be filed down. This was to give room for CCF's to move together with the thermoplastic filament. Once the hole has been made in the PTFE bowden tube another snippet of PTFE tubing needs to be cut which will be pushed into the

radiator and slightly into the heat break, aligning the PTFE tubes. The printing configuration with the PTFE tubes connected can be seen in Figure 35a. An example where CCF's have been fed through the extruder driver and PTFE tubing for the CCF which leads into the PTFE tubing for the thermoplastic and finally out of the nozzle can be seen in Figure 35b.



(a) The CCF path shown going through the radiator out of the nominal bowden PTFE tubing for the thermoplastic. The path is illustrated with a metal wire which was also used to align the holes in the two PTFE tubes.



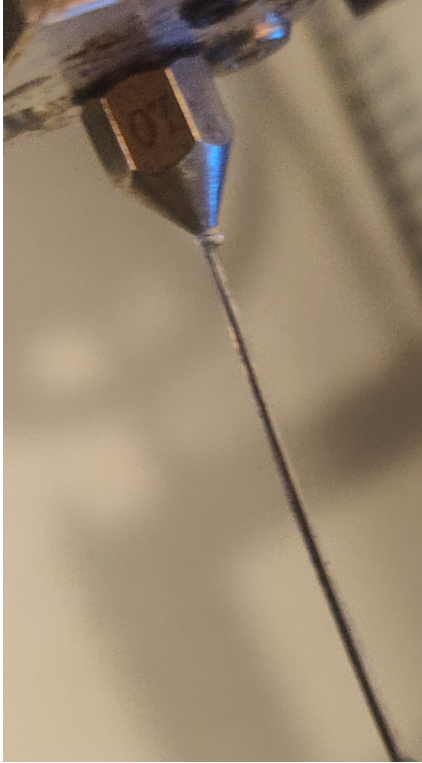
(b) CCF being fed from the extruder driver out from the nozzle with a backing plate holding the extruder driver driver stepper motor behind it in place.

Figure 35: The paths that the CCF takes.

The backing plate used was also used an early prototype of attaching motors to the end effector and test weight tolerances of the end effector. No degradation in quality was seen with the backing plate attached. Making sure that the PTFE tubing

could be aligned not only with the drill hole in the end effector but also the extruder driver was tested using the backing plate prototype.

Metal wire was used to align the holes and the radiator was clamped along the ridges bending the metal slightly to keep the CCF PTFE tubing in place and aligned. Making the connection was difficult but once the PTFE tubes were locked in place with the nozzle as well the connection of the tubes remained reliable. Due to only aligning the tubes and the lack of a mechanical connection means that with some level of force the holes could be misaligned. The CCF PTFE tubing should not experience large forces during the printing, but a mechanical connection for future iterations should be preferred for better reliability. With the nozzle in place and CCF's fed into the PTFE tubing, the PLA was extruded through driving the filament in at the extruder driver. When the PLA filament moved through the nozzle, the CCF followed as well. The capability to extrude PLA and dry CCF into one consolidated extrusion has been demonstrated with this proof of concept. The extrusion of the CCF's through the nozzle can be seen in Figure 36a. The resulting material is a very stiff CCF reinforced PLA. The CCF's adheres to the PLA and was not possible to remove after the print. The resulting CCF reinforced PLA can be seen in Figure 36b.



(a) PLA and CCF's extruded through the *Ender 3* nozzle.



(b) The extruded strand of CCF reinforced PLA printed with the *Ender 3* in Figure 36a.

Figure 36: 3D printed CCF and PLA.

The extrusion test of CCF reinforced PLA with the *Ender 3* 3D printer was highly successful and gives good confidence to continue the design utilising CCF's as the sensing material.

4.3 Non-Planarity

For the non-planarity an open source *Python* script was used which was originally sourced from a *GitHub* repository, only tweaking the user controls as defined in the script [10]. The script works through taking Marlin flavored G-Code as an input. Within the script a spline defines a new non-planar path for the part adding Z-axis movements throughout the movement path as well as controlling the extrusion rates for the concave and convex parts which need to be change for non-planar printing. Relative extrusion needs to be used in the script. Figure 37a shows the original

sliced file, 37b shows the spline for which the altered G-Code should follow and 37c shows the end result in the G-Code viewer.

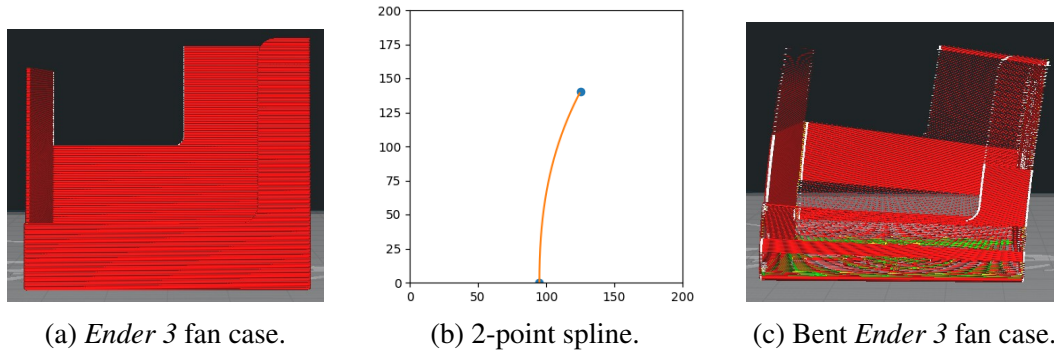


Figure 37: *Ender 3* fan case used to illustrate the feasibility of non-planar printing with the COTS *Ender 3* 3D printer.

Ultimaker Cura 4.11.0 and other slicer software's are only capable of defining movements in planar layers, which means that they have a difficult time visualizing non-planar parts, which is why the fan case is semi-transparent. The spline that the bent G-Code follows is defined in Listing 6 which defines the points seen in blue in Figure 37b.

Listing 6: 2-point spline that defines how the model should be bent.

```
SPLINE_X = [95 , 125]
SPLINE_Z = [0 , 140]
```

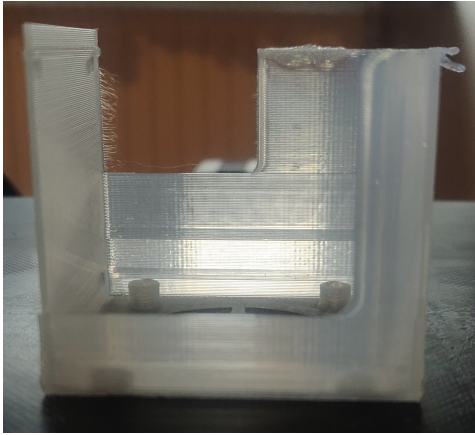
The resulting G-Code file will have Z-axis movements in almost every line of code. An example of how the movement now looks can be seen in Listing 7.

Listing 7: Non-planar commands of the *Ender 3* fan case model.

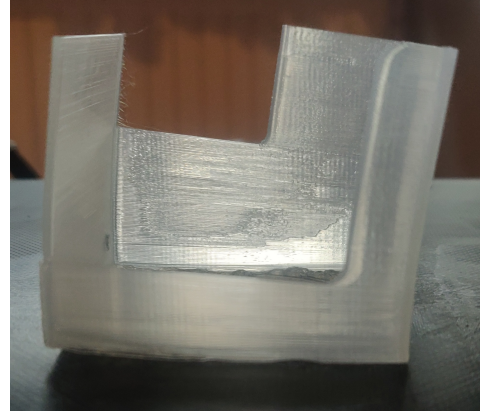
```
G1 X94.34795 Y140.11 Z22.733 E0.00838
G1 X94.2141 Y139.951 Z22.739 E0.00694
G1 X94.19612 Y139.843 Z22.74 E0.00365
G1 X94.19612 Y97.35 Z22.74 E1.41765
G1 X94.59569 Y97.35 Z22.721 E0.01333
G1 X94.59569 Y140.15 Z22.721 E1.42655
```

In Figure 38a the normal *Ender 3* fan case which has been printed in PLA can be seen. SolidWorks blueprints for an easy print fan case can be seen in Appendix C. It is a modified version of the original *Ender 3* fan case provided in the *Ender 3* model

seen in Appendix G. The fan case has been modified to not need any supports and lower the risk of the part hitting the fan case when being printed with a non-planar method. A non-planar fan case test print using the non-planar script with the spline in Listing 6 can be seen in Figure 38b.



(a) *Ender 3* fan case printed in PLA.



(b) A non-planar print of an *Ender 3* fan case printed in PLA.

Figure 38: *Ender 3* fan case before and after the bending.

The non-planar printed fan case illustrates the feasibility of utilising non-planar 3D printing with the *Ender 3* at shallow angles. For less shallow angles the fan shroud and heating block may need to be modified.

4.4 Conclusion

The tests and manufacturability analysis of the current configuration of 3D printer and material were conceptually simple but more difficult when actually implemented. The successes of the analysis will be used as the basis for the software and hardware design.

4.4.1 Materials

Due to the success of the filament and extrusion test the material that will be utilised as the sensor is dry CCF's. The mechanical properties of dry CCF's are good and the fibre's are commonly used as the piezoresistive material in self-sensing materials. PLA has a high level of printability and several sources utilise it as the polymer matrix for the sensor structure when using CCF's as the sensor. That combined with the fact that the extrusion test was successful with PLA, the polymer matrix of

choice for the design will also be PLA thermoplastic with a diameter of 1.75 mm.

4.4.2 Manufacturing Method

The manufacturing method with the fewest downsides whilst not being too difficult to implement is a traditional FDM 3D printer operating non-planar G-Code. The traditional FDM 3D printer has a lot of literature, guides and open source content either community made or produced by the manufacturer. The non-planar element of the additive manufacturing platform has already been proven. Having the freedom of both printing in the plane as is while being able to print in a non-planar way through software and minute hardware modifications means that the manufacturing method shows a lot of flexibility together with a low threshold of implementation complexity. Having dry CCF's be printed on a traditional 3D printer with non-planar G-Code is also completely novel, which further encourages the non-planarity in the design.

5 Design

The design is based off the promising results of the filament and extrusion tests of the manufacturability analysis. The CCF feeding mechanism with the PTFE tubing going through the radiator and heat break will remain the same, joining the CCF and thermoplastic at the wall of the heat break. In situ curing is the method of printing that will be used inspired by existing design benchmarks. Actual curing of the fibre is not necessarily a goal and the level of curing can not be measured with the hardware available, hence the term in situ adhesion will be used. That is due to the adhesion between fibre and thermoplastic already having been proven for the current printing configuration. The 3D printer that will be used as the base for the design is the *Creality Ender 3*. But the design philosophy can be used on almost any COTS single nozzle 3D printer with minor modifications to the dimensions of the backing plate with regards to screw positions and outer geometry. SolidWorks was the CAD software for modeling the end effector. Measuring and evaluating dimensions as well as testing the fit through CAD was done with the help of a CAD model of the *Ender 3 G*. The assembled CAD model can be seen in Figure 39.

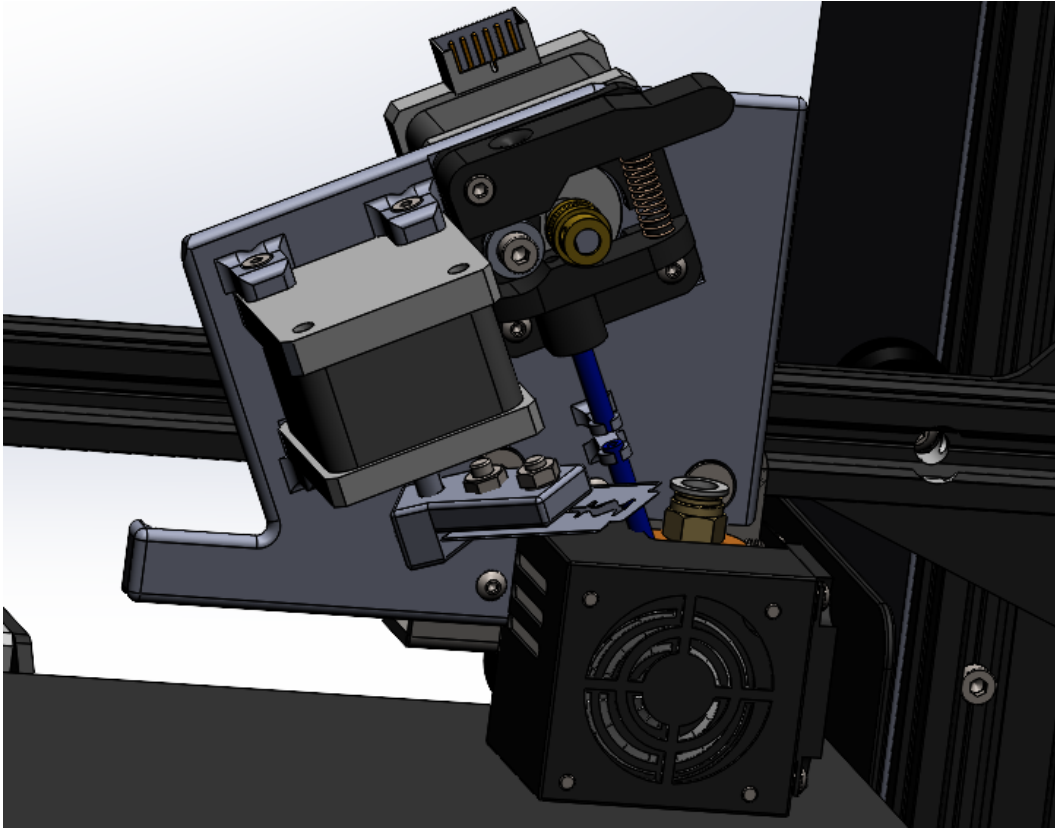


Figure 39: Design for the end effector.

Interpreting basic Marlin flavor G-Code must be possible for the 3D printer as well as it having to be able to use relative extrusion in the G-Code. The real-world counterpart fit test can be seen in Figure 40.

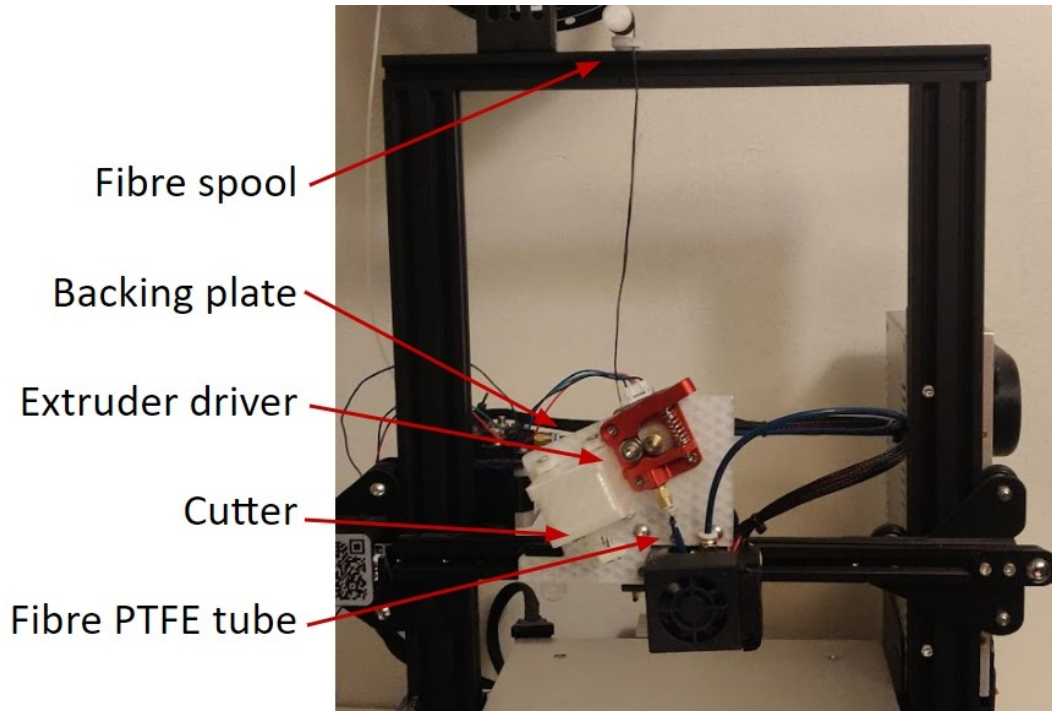


Figure 40: A fit test and overview of parts that will be presented as a mix of 3D printed parts together with real parts if they could be attained.

5.1 Material

The CCF tow used is a 3K tow from *Easy Composites EU*. The tow is pulled in half to provide roughly 1500 filaments in one carbon fibre tow. The specifications for the 3K carbon fibre tow can be seen in Table 2.

Table 2: Specifications of the 3K CCF filament [8].

Number of filaments	Diameter	Tensile Strength	Tensile Modulus	Elongation at Break	Density
3000	7 μm	4120 MPa	234 GPa	1.8 %	1.79 g/cm ³

The thermoplastic used as the structural part will be PLA with a diameter of 1.75 mm due to the success of both the extrusion and filament test in the manufacturability analysis when using it.

5.2 Backing Plate

A direct drive extruder will be used for the feeding of CCF into the nozzle. A cutter also needs to be positioned to cut the CCF. Both the extruder driver and cutter will be positioned close to the end effector of the 3d printer, which requires everything to be attached to an external backing plate. COTS modification's for converting the 3d printer into a direct drive system exists which mount onto the fan case. However, due to having to add space for a motor for driving the fibre as well as cutting of the fibre's, COTS options don't exist for a two motor configuration. A custom 3d printed PLA backing plate will be attached to the fan mount of the *Ender 3*. Using a 3d printed structure will also have the benefit of being very low weight which is better for a 3d printer end effector. For future design iterations a machined aluminium backing plate could be preferred if degradation of the backing plate was to be experienced. For now the printer is capable of printing with the backing plate and weight of two motors and the extruder driver. Quality of the print will often be affected when weight is added to the end effector, a way to combat this is through lowering the printing speeds. An image of the backing plate can be seen in Figure 41.

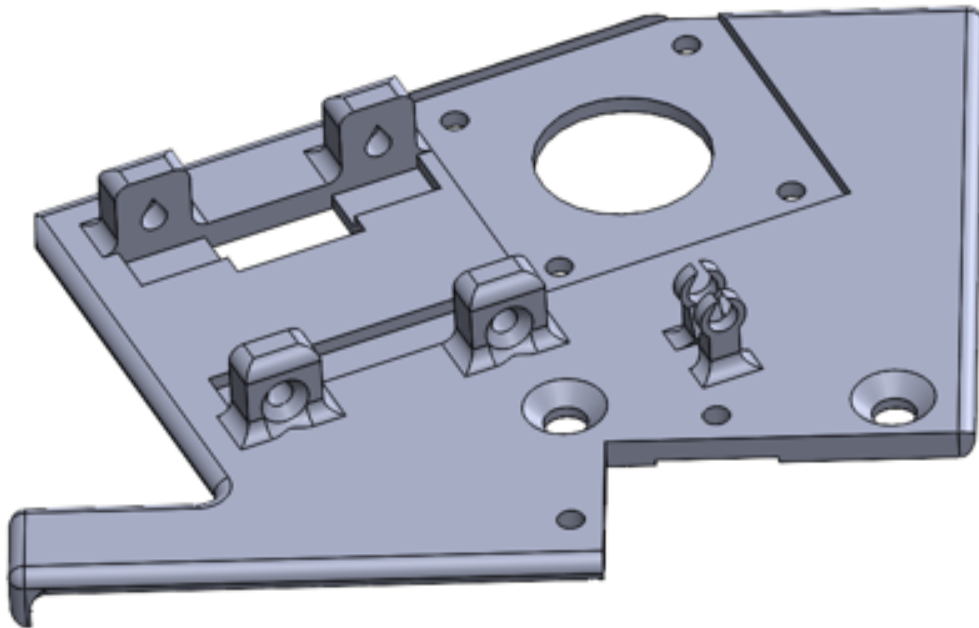
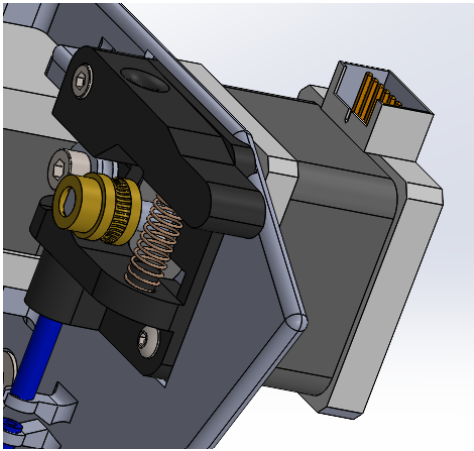


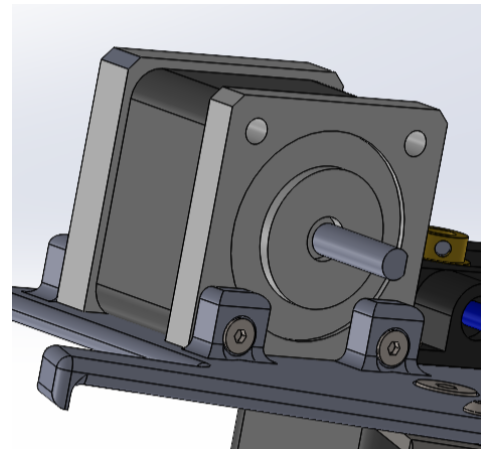
Figure 41: Backing plate which will house the CCF printing components.

The backing plate includes a protrusion towards the left lower side which is used to

activate a switch when the *Ender 3* is zeroing It's axes. If it was not included the end effector with It's new dimensions would hit the left rail of the *Ender 3* frame. An unfortunate affect that the new dimensions of the end effector have is that the X coordinate is 55.5 mm shorter. The nominal build area of the 3D printer is 235 x 235 mm but is now limited to 179.5 x 235 mm. The complete blueprints for the backing plate can be seen in Appendix B. The extruder driver stepper motor together with the extruder driver mechanism and the cutter stepper motor attached to the backing plate can be seen in Figure 42.



(a) Extruder driver and It's stepper motor on the backing plate.



(b) Cutter stepper driver without cutter arm.

Figure 42: The continuous pathing cube model showing compatible and incompatible tool paths.

A real-world fit test has been implemented with a mix of 3D printed parts and real hardware to validate the assembly of the backing plate onto the 3D printer, and components onto the backing plate which can be seen in Figure 43.

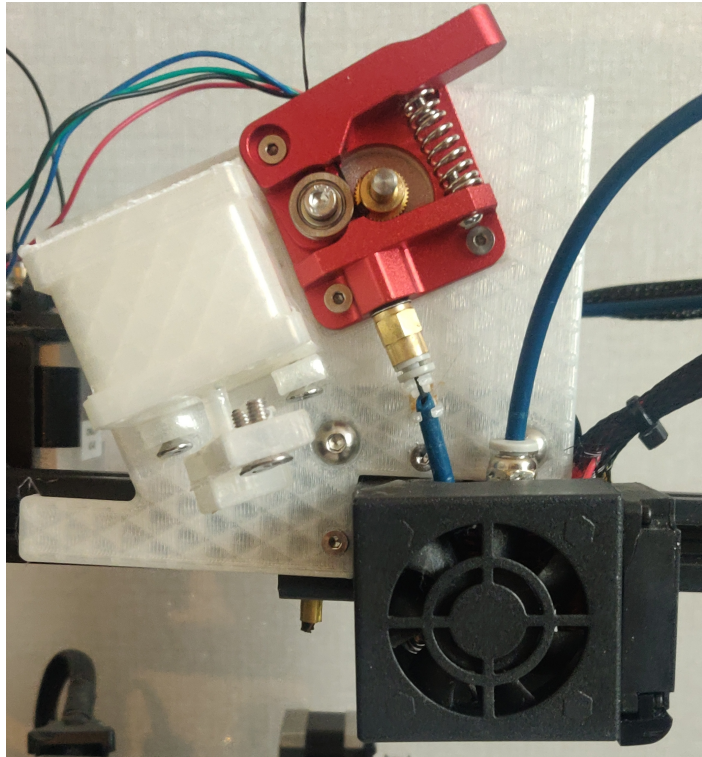


Figure 43: Fit test of the backing plate validating It's dimensions.

The CCF can be seen entering the extruder driver and also entering the blue PTFE tubing from where it enters the nozzle.

5.3 Fibre Spool

The CCF filament needs to be held at a slight tension in the fibre spool and at a distance from the printer nozzle and moving parts, much like traditional filament spools. The filament spool can be seen in Figure 44 for which the blueprints can be seen in Appendix D.

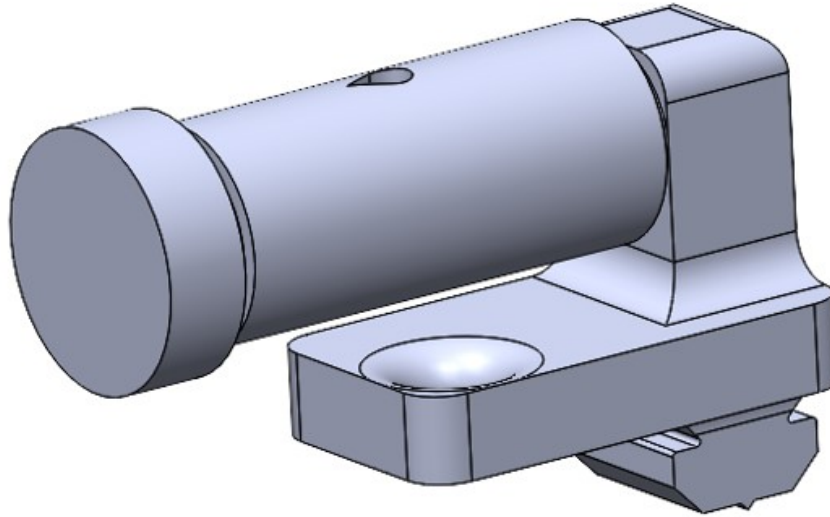


Figure 44: Fibre spool for the CCF.

The design consists of three parts and uses a freely rotating tube which rotates on a cylinder and stays locked in place by a friction fit tap that gets put on afterwards. The tube has slight friction on the cylinder which acts as the tensioning system. The bracket for holding the cylinder is modeled after the *Ender 3* rails and slots in. Both the tube and the cylinder have a tear drop shaped hole going through them. It serves as a pressure release when the tap is installed but also holds on to the CCF end. When installing the CCF to the spool the fibre should be put through the hole through the tube and cylinder, where after the tap should be inserted so that it grips the fibre tightly. Doing this ensures that the fibre's won't fall of the spool, and there's no need to use tape or other adhesives keeping the fibre in place. The filament spool attached to the *Ender 3* with CCF's applied can be seen in Figure 45.

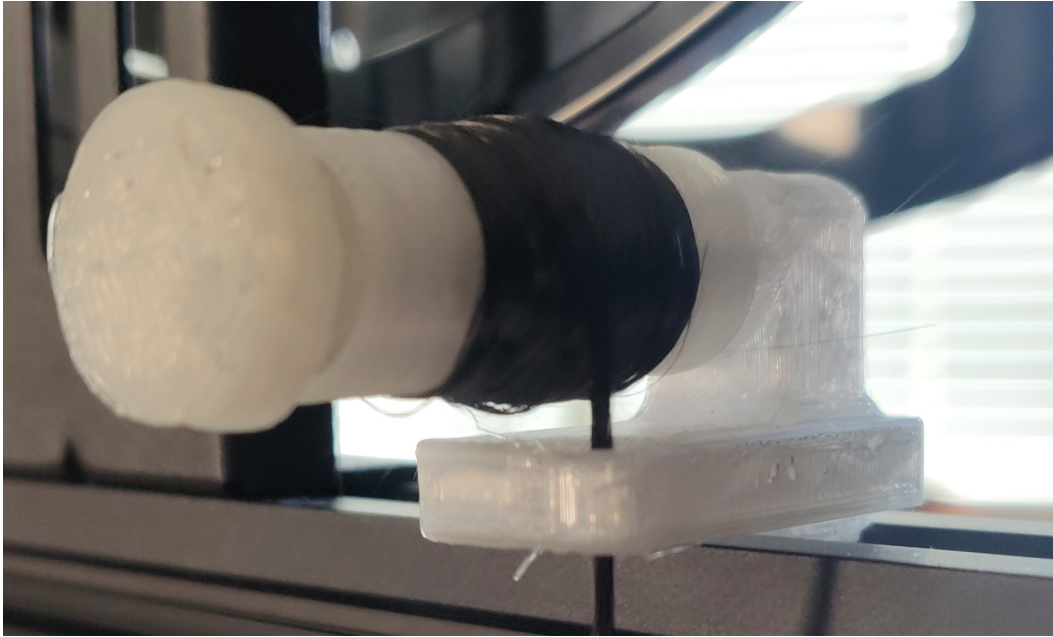


Figure 45: Carbon fibre filament spool holding 2.5 m of 1.5K carbon fibre tow.

The attachment mechanism turned out very stable as the *Ender 3* rails grips the base of the spool, as well as the spool providing a consistent tension when the filament is being pulled.

5.4 Fibre Extrusion

The extruder driver is a generic *Ender 3* extruder driver and is attached to the backing plate together with its motor with four M3 screws. The modifications needed is to utilise a larger cog wheel due to the CCF strands being very thin compared to 1.75 mm PLA filament for which it is designed. The direct drive extruder also keeps the tension between the fibre spool and extruder driver gripper. This is due to the necessity of having the final tensioning node of the filament positioned close to the nozzle which minimizes the chance of buckling of the CCF's between the extruder driver and nozzle. An aftermarket *Ender 3* COTS extruder driver a 42-40 stepper motor capable of driving it has been used as the basis for the dimensions and attachment points of the backing plate. The extruder driver for the CCF needs to be powered by a separate stepper motor not included in the *Ender 3* 3D printer. The thermoplastic will be driven with an extruder driver that is positioned away from the nozzle on the frame of the 3D printer which is the manufacturer's configuration. The extruder driver will feed the CCF's through the PTFE tube as was done in the

extrusion test of the manufacturability analysis. The drill hole in the CAD model has been positioned in the same way as the real world drill hole which was at an angle of 25°. A SolidWorks section view of the PTFE tube inserted into the radiator can be seen in Figure 46.

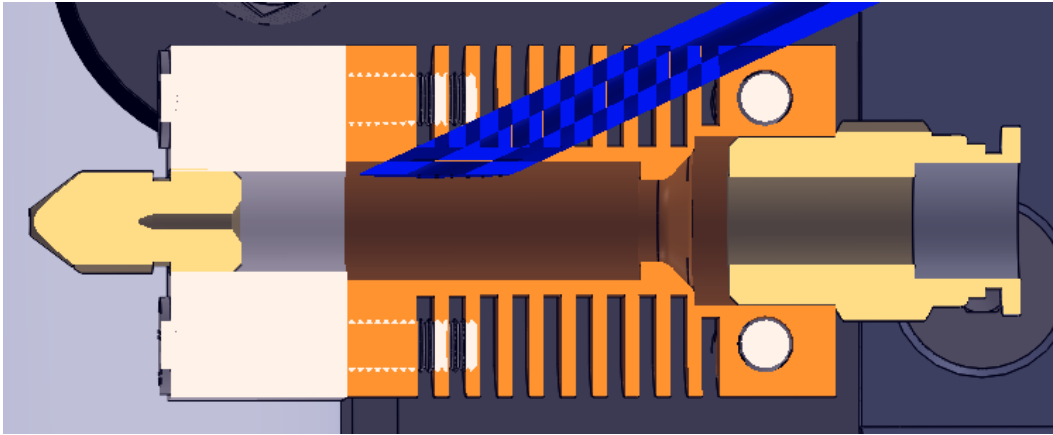


Figure 46: A section view of the radiator, nozzle and heating block with the CCF PTFE tubing inserted.

5.5 Feeding of CCF

The feeding of fibre is done through a PTFE tube with a slit in it where the fibre has to be cut. The first part of the tube ends just before the cutter system and sits in a coupling arm and the second part of the tube ends just after the cutter system and sits in another coupling arm. The arms hold the tubes aligned and close so that the fibre can flow from one tube to the other. The PTFE tubing is *CAPRICORN Premium XS Series Dark Blue Tubing* which can tolerate PLA printing temperature's allowing the tube to be inserted into the heating block without degradation or off-gassing of the PTFE tubing [58]. An example of the PTFE tube installed in the coupling arms can be seen in Figure 47.



Figure 47: Feed tube coupling brackets.

Due to the hardness of CCF's a hardened steel nozzle will be utilised instead of the included and typically used brass nozzle. These are available COTS and screws on to the *Ender 3* end effector. The nominal nozzle diameter for the *Ender 3* is 0.4 mm, but to limit buckling in the nozzle and follow the extrusion test of the CCF, a larger 1 mm nozzle was installed. A larger nozzle also allows for faster 3D printing and larger margins for extruding both fibre and thermoplastic through the same nozzle, however parts do get less precise and get larger layer lines. When both fibre and thermoplastic are being extruded the nozzle can not extrude the same amount of thermoplastic, which has to be accounted for in the G-Code.

5.6 Feeding of Thermoplastic

The feed tube for the thermoplastic will be the included PTFE bowden tube which is the nominal way of feeding thermoplastics from the filament spool to the nozzle for the *Ender 3* 3D printer. The filament guide, together with the extruder driver for the thermoplastic will be left as is. Converting the thermoplastic extruder driver into a direct drive system was considered as well, but adding another motor onto the print head would mean an even heavier end effector which could cause a degradation of print quality, especially at higher print speeds. The only modification that had to be made to the thermoplastic PTFE tubing is filing of the inner diameter of the tubing between where the nozzle is and where the fibre tubing intersects the thermoplastic tubing. The filing has to be done to slightly increase the inner dimension of the tube allowing for the fibre to travel along the thermoplastic tubing out through the nozzle.

5.7 Cutting of CCF

The cutter works by utilising the slit in the CCF filament guide which can be seen in Figure 47. A cutting arm operated by a stepper motor attached to the backing plate through four M3 screws will cut the carbon fibre. The motor for the cutting arm is attached to the backing plate and the cutting arm is attached directly to the motor. The cutting arm is just the holder for a generic razor blade that gets screwed on by two M4 bolts with a nut on the end of both bolts. The cutter arm is attached to the stepper motor through a M3 bolt which is screwed on so it contacts the flat part of the rotor. A CAD image of the assembled cutter arm can be seen in Figure 48.

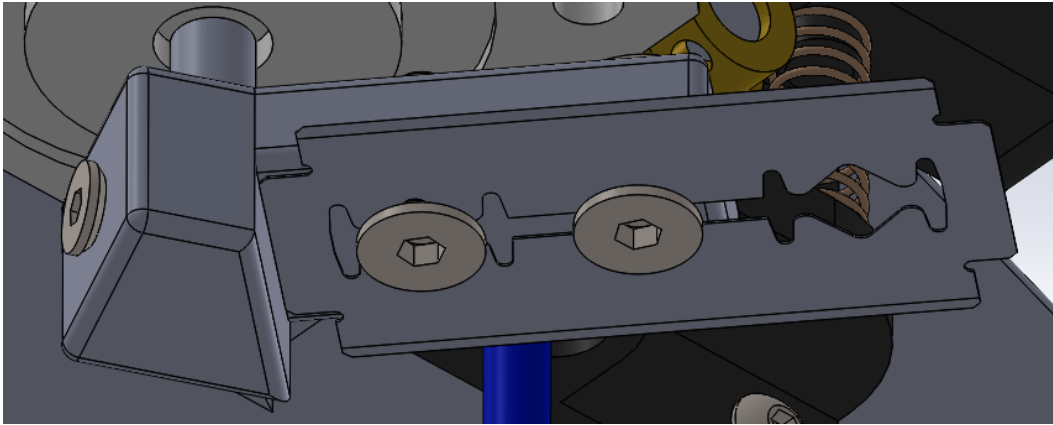


Figure 48: Cutter arm with the razor blade attached and bolts for the razor blade and cutter arm.

When the motor rotates the razor blade slices the CCF between the PTFE tubing brackets and then moves back to the original position waiting for the next command for the next fibre cut command.

5.8 Software Design

The software design consists of a way of slicing the part, e.g. generating the generic G-Code. Continued by G-Code for fibre path optimization and finally adding non-planarity into the G-Code.

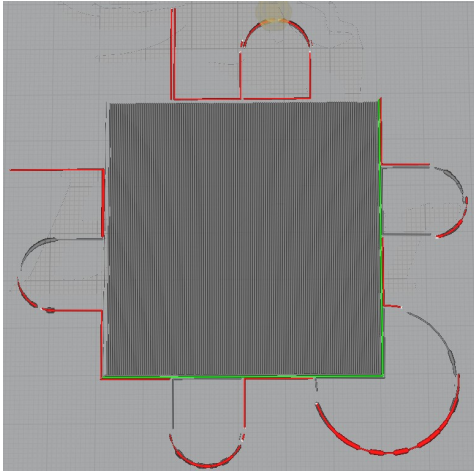
5.8.1 Slicing

When printing a part the process has to start with any generic slicer software capable of enabling relative extrusion. Just like in the manufacturability analysis, *Ultimaker*

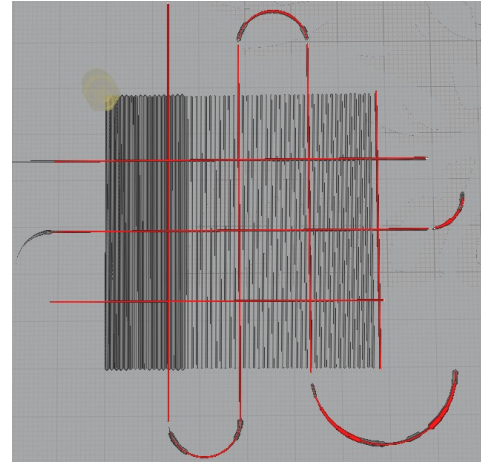
Cura 4.11.0 will be the slicer of choice. The nozzle temperature is generally governed by the PLA melting temperature and the material manufacturer specifications of their PLA filament. The temperature is chosen so that the thermoplastic is soft but not melted at the point of contact with the fibre. That allows the fibre to travel by friction with the thermoplastic to the nozzle. The temperature that worked best in the manufacturability analysis was a temperature of 220°C which is around 40°C above the melting temperature of PLA. The speed at which the PLA and fibre could be extruded reliably is around 20 mm/s. Filament retraction which pulls back the thermoplastic when changing positions in the print to minimize strings of material between objects has been disabled to not pull up the fibre through the nozzle. The G-Code line M83 needs to be inserted in beginning of the G-Code as well to enable relative extrusion. In the case that the print should be non-planar, the G-Code file needs to be saved in the same folder as the non-planar script is.

5.8.2 Continuous Fibre Placement

To place continuous fibre's the end effector has to have a continuous print path for segments of CCF. It's achieved through manually altering an outer layer path in the G-Code to have continuous motion, as in the manufacturability analysis. The software used for G-Code manipulation was *Notepad++* together with *Repetier-Host 2.2.4* for exact visualization of the print path. A non-path-optimized print using the model seen in Appendix F can be seen in Figure 49a and a path optimized version can be seen in Figure 49b where the initial motion of the end effector is a continuous motion shown by the red color.



(a) The *Ultimaker Cura 4.11.0* slicer generated continuous fibre placement incompatible G-Code visualized.



(b) The *Ultimaker Cura 4.11.0* slicer generated path in Figure 49a modified for continuous fibre placement.

Figure 49: The continuous pathing cube model showing compatible and incompatible tool paths.

Ultimaker Cura 4.11.0 has difficulty displaying non-planar G-Code, which is why it looks like there are gaps in the continuous path.

5.8.3 Non-Planarity

Once the continuous path-optimized G-Code is generated, the same non-planar script as seen in the manufacturability analysis [10] is used for implementing the non-planarity. A spline which defines the level of non-planarity, as well as the layer height is defined in the script. After the script is executed and a non-planar G-Code file is generated it can now be printed.

A part using non-planar 3D printing and manual lay up of CCF can be seen in Figure 50.

5.9 Future Work

Future work with the literature review and the filament and extrusion test as the base can be done to further improve the design. Increasing the functionality through design iterations can be the continued work. Suggested iterative design process following the design process already used as a reference can be seen in Figure 52.

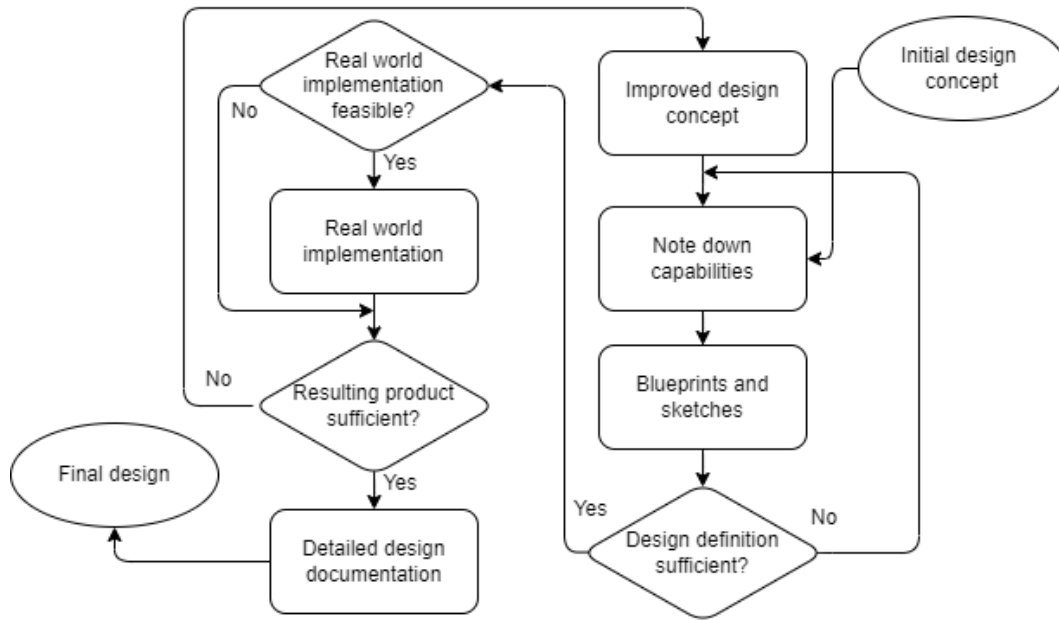


Figure 52: Iterative hardware design approach.

The initial design concept was the dry CCF extrusion of a planar FDM 3D printer and the requirements for it should be defined and then redefined in the case of a later design iteration. On the following design iterations the requirement of passing will be a comparison of the previous iteration to the current. So a trade-off analysis shall be made for which the combination of the manufacturing device and its capabilities need to be greater than the previous iteration. Here, taking the different performance indices such as time, money and reliability into account will determine the failure or success of a design iteration. The design definition follows a more stringent set of requirements. Due to the device not being able to be manufactured without well defined parts, dimensions and specifications the design definition needs to be well defined and follow the following criteria.

1. Capabilities defined (degrees of freedom, extrusion mechanism)
2. Dimensions defined

3. Parts labeled

Once the design definition meets the following criteria, a consideration of a real world implementation should be done. This step requires outreach to institutions, mainly LTU that have materials and hardware available. It may require purchasing of parts or utilising what already exists. Having an idealized conceptual design may work while the real world implementation will not. Fit testing parts can be done through 3D printing the design which will likely be a helpful and validating step of the design as have been done throughout the current design.

The software to use will follow an iterative design approach as well. For the first iteration the generation of the 3D printed part a slicer software will be utilised. For the motor feeding the sensor into the extrusion mechanism additional slicer commands need to be implemented. For the later iterations of the hardware design the software design needs to progress in parallel. The 5-axis printing would need constant communication between the rotating bed gantry and the printer. While a robotic arm software would need completely custom slicer software separate from what a traditional planar FDM 3D printer slicer uses. The general conceptualized workflow for the software design can be seen in Figure 53.

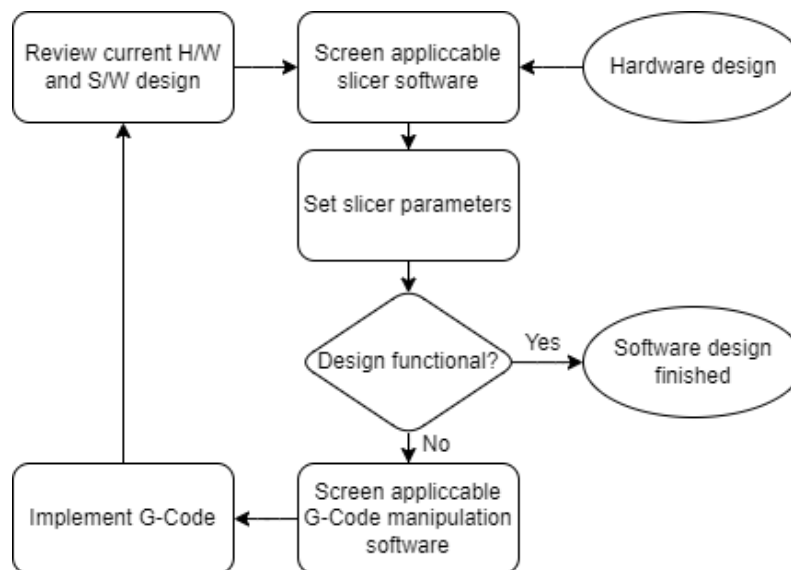


Figure 53: Iterative design process of software with the hardware design as input.

6 Conclusion

What was sought after was to provide a design capable of printing a self-sensing part, end-to-end. All parts of the goal have been covered, however the integration between the parts has not has a working real-world example due to hardware limitations and integration difficulties. The design is capable of producing CCF reinforced PLA acting as a self-sensing material. The extrusion of fibre together with thermoplastic has been achieved successfully, whilst a part without manual placement or help has not been achieved. Novelty in having a FDM 3D printer capable of printing dry CCF through a single nozzle in situ adhesion with full freedom of the tool pathing used to apply it on fibre-optimized non-planar 3D printing is achieved. The extrusion of dry CCF has been validated, the possibility of non-planar printing and adhesion of CCF to an additively manufactured non-planar PLA part has been validated. A tool pathing method for CCF printing has been presented in the design. The design shows promise but further testing and a real world implementation of the 3D printer should be performed. Following the iterative hardware and software workflow can increase the functionality of the additive manufacturing hardware and software, while also increasing the novelty factor. Having the 3D printer capable of making a real-world part, and then integrating things like 5-axis printing or a robot arm to even further increase the functionality and novelty factor of the design.

Having proven the capabilities of a cheap COTS 3D printer to be able to perform all of the functionalities individually has been one of the main results. Doing it with hardware worth roughly 200 € is one of the significant results. The literature review including all of the functionalities mentioned and implementable by researchers or industry further validates the possibility of a real-world implementation. A full proof of concept has been implemented, but further refinements are needed in the integration of all parts.

Future Work

For future iterations of the filament spool a elastic or spring tension could be added as well. When reliability is improved a smaller nozzle diameter could be used. Heavily modifying the geometries of the COTS end effector and building a different backing plate may produce an end effector that does not limit the print size. Modifications could be made to the fan case and an extended nozzle implemented to increase the angle of non-planarity that the printer can print. Having a main board capable of driving two extra motors means that the implementation of the extruder driver for the CCF and the cutter of the CCF can be implemented as well. A solution utilising digital twin reinforcement learning could be a way to create a

software algorithm that generates the G-Code for the sensor placement. If a simulation can be made with the placement and have a learning algorithm learn from it, a large software programming part could be automated. With time the solutions provided by the algorithm might produce a better self-sensing material than what can be done through user defined sensor placements [46].

References

- [1] Daniel Ahlers et al. “3D printing of nonplanar layers for smooth surface generation”. In: *2019 IEEE 15th International Conference on Automation Science and Engineering (CASE)*. IEEE. 2019, pp. 1737–1743.
- [2] Saeed Akbari et al. “Large-Scale Robot-Based Polymer and Composite Additive Manufacturing: Failure Modes and Thermal Simulation”. In: *Polymers* 14.9 (2022), p. 1731.
- [3] N Angelidis, CY Wei, and PE Irving. “The electrical resistance response of continuous carbon fibre composite laminates to mechanical strain”. In: *Composites Part A: applied science and manufacturing* 35.10 (2004), pp. 1135–1147.
- [4] Rafael Vidal Aroca et al. “Sequential additive manufacturing: automatic manipulation of 3D printed parts”. In: *Rapid Prototyping Journal* (2017).
- [5] DG Bekas et al. “3D printing to enable multifunctionality in polymer-based composites: A review”. In: *Composites Part B: Engineering* 179 (2019), p. 107540.
- [6] Ismayuzri Bin Ishak, Joseph Fisher, and Pierre Larochelle. “Robot arm platform for additive manufacturing using multi-plane toolpaths”. In: *International Design Engineering Technical Conferences and Computers and Information in Engineering Conference*. Vol. 50152. American Society of Mechanical Engineers. 2016, V05AT07A063.
- [7] Alex M Boulger et al. *Pick and place robotic actuator for big area additive manufacturing*. Tech. rep. Oak Ridge National Lab.(ORNL), Oak Ridge, TN (United States), 2018.
- [8] *Carbon Fibre Tow 3K, 6K and 12K sizes*. Easy Composites EU B.V. 2022. URL: <https://media.easycomposites.co.uk/datasheets/Carbon%5C%20Fibre%5C%20Tow>.
- [9] Josef F Christ et al. “3D printed highly elastic strain sensors of multiwalled carbon nanotube/thermoplastic polyurethane nanocomposites”. In: *Materials & Design* 131 (2017), pp. 394–401.
- [10] CNCKitchen. *GCodeBending*. 2022. URL: <https://github.com/CNCKitchen/GCodeBending>.
- [11] Adam Cohen et al. *Additive manufacturing of active devices using dielectric, conductive and magnetic materials*. US Patent 10,254,499. Apr. 2019.

- [12] Michael Dawoud, Iman Taha, and Samy J Ebeid. “Strain sensing behaviour of 3D printed carbon black filled ABS”. In: *Journal of Manufacturing Processes* 35 (2018), pp. 337–342.
- [13] Andrew N Dickson, Keri-Ann Ross, and Denis P Dowling. “Additive manufacturing of woven carbon fibre polymer composites”. In: *Composite Structures* 206 (2018), pp. 637–643.
- [14] Martin Eichenhofer, Joanna CH Wong, and Paolo Ermanni. “Continuous lattice fabrication of ultra-lightweight composite structures”. In: *Additive Manufacturing* 18 (2017), pp. 48–57.
- [15] David Espalin et al. “3D Printing multifunctionality: structures with electronics”. In: *The International Journal of Advanced Manufacturing Technology* 72.5 (2014), pp. 963–978.
- [16] Rouhollah Dermanaki Farahani et al. “Direct-write fabrication of freestanding nanocomposite strain sensors”. In: *Nanotechnology* 23.8 (2012), p. 085502.
- [17] Urban Fasel et al. “Composite additive manufacturing of morphing aerospace structures”. In: *Manufacturing Letters* 23 (2020), pp. 85–88.
- [18] Andreas Fischer et al. *Tool and method for sheathing an elongate product available by the meter*. US Patent App. 14/421,651. 2015.
- [19] Andrew Gleadall. “FullControl GCode Designer: open-source software for unconstrained design in additive manufacturing”. In: *Additive Manufacturing* 46 (2021), p. 102109.
- [20] Karthikeyan Gnanasekaran et al. “3D printing of CNT-and graphene-based conductive polymer nanocomposites by fused deposition modeling”. In: *Applied materials today* 9 (2017), pp. 21–28.
- [21] Elliott R Griffiths and Simon J Leigh. “Multi-material fused deposition modelling for integration of interdigital dielectric sensors into carbon fibre composite tooling for in process cure monitoring”. In: *Sensors and Actuators A: Physical* 296 (2019), pp. 272–277.
- [22] Øyvind Kallevik Grutle. “5-axis 3D Printer”. MA thesis. 2015.
- [23] E Häntzsche et al. “Characteristics of carbon fiber based strain sensors for structural-health monitoring of textile-reinforced thermoplastic composites depending on the textile technological integration process”. In: *Sensors and Actuators A: Physical* 203 (2013), pp. 189–203.
- [24] Freddie Hong et al. “Open5x: Accessible 5-axis 3D printing and conformal slicing”. In: *arXiv preprint arXiv:2202.11426* (2022).

- [25] Alexander Horoschenkoff, Tobias Mueller, and Andreas Kroell. “On the characterization of the piezoresistivity of embedded carbon fibres”. In: *ICCM 17th* (2009).
- [26] Huang Huang, Caiqian Yang, and Zhishen Wu. “Electrical sensing properties of carbon fiber reinforced plastic strips for detecting low-level strains”. In: *Smart materials and structures* 21.3 (2012), p. 035013.
- [27] M Ibrahim et al. “Resistivity study on conductive composite filament for freeform fabrication of functionality embedded products”. In: *ARPJ Journal of Engineering and Applied Sciences* 11.10 (2016).
- [28] John Irwin et al. “The RepRap 3-D printer revolution in STEM education”. In: *360 of Engineering Education* (2014).
- [29] Jingchao Jiang, Stephen T Newman, and Ray Y Zhong. “A review of multiple degrees of freedom for additive manufacturing machines”. In: *International Journal of Computer Integrated Manufacturing* 34.2 (2021), pp. 195–211.
- [30] Carl J Johnston et al. “Pulmonary effects induced by ultrafine PTFE particles”. In: *Toxicology and applied pharmacology* 168.3 (2000), pp. 208–215.
- [31] Nataliya Kalashnyk et al. “Monitoring self-sensing damage of multiple carbon fiber composites using piezoresistivity”. In: *Synthetic Metals* 224 (2017), pp. 56–62.
- [32] Hang-Gyeom Kim et al. “Additive manufacturing of high-performance carbon-composites: An integrated multi-axis pressure and temperature monitoring sensor”. In: *Composites Part B: Engineering* 222 (2021), p. 109079.
- [33] Kyuyoung Kim et al. “3D printing of multi-axial force sensors using carbon nanotube (CNT)/thermoplastic polyurethane (TPU) filaments”. In: *Sensors and Actuators A: Physical* 263 (2017), pp. 493–500.
- [34] Takafumi Kobayashi et al. “Electrically Conductive Polymer Nanocomposites for 3D Printing”. In: *ECS Meeting Abstracts*. 3. IOP Publishing. 2018, p. 192.
- [35] S Koda and H Tanaka. “Direct G-code manipulation for 3D material weaving”. In: *Nanosensors, Biosensors, Info-Tech Sensors and 3D Systems 2017*. Vol. 10167. SPIE. 2017, pp. 215–221.
- [36] Joseph R Kubalak, Alfred L Wicks, and Christopher B Williams. “Using multi-axis material extrusion to improve mechanical properties through surface reinforcement”. In: *Virtual and Physical Prototyping* 13.1 (2018), pp. 32–38.

- [37] Simon J Leigh et al. “A simple, low-cost conductive composite material for 3D printing of electronic sensors”. In: *PloS one* 7.11 (2012), e49365.
- [38] Nanya Li et al. “Path-designed 3D printing for topological optimized continuous carbon fibre reinforced composite structures”. In: *Composites Part B: Engineering* 182 (2020), p. 107612.
- [39] Mingjie Liu et al. “Research of a novel 3D printed strain gauge type force sensor”. In: *Micromachines* 10.1 (2018), p. 20.
- [40] Congcong Luan et al. “Large-scale deformation and damage detection of 3D printed continuous carbon fiber reinforced polymer-matrix composite structures”. In: *Composite Structures* 212 (2019), pp. 552–560.
- [41] Congcong Luan et al. “Self-sensing of position-related loads in continuous carbon fibers-embedded 3D-printed polymer structures using electrical resistance measurement”. In: *Sensors* 18.4 (2018), p. 994.
- [42] Gregory Thomas Mark and Antoni S Gozdz. *Apparatus for fiber reinforced additive manufacturing*. US Patent 9,579,851. Feb. 2017.
- [43] Fatemeh Mashayekhi et al. “Fused Filament Fabrication of Polymers and Continuous Fiber-Reinforced Polymer Composites: Advances in Structure Optimization and Health Monitoring”. In: *Polymers* 13.5 (2021), p. 789.
- [44] *MATERIAL DATASHEET Composites*. Markforged. 2021. URL: <http://static.markforged.com/downloads/composites-data-sheet.pdf>.
- [45] Ryosuke Matsuzaki et al. “Three-dimensional printing of continuous-fiber composites by in-nozzle impregnation”. In: *Scientific reports* 6.1 (2016), pp. 1–7.
- [46] Marius Matulis and Carlo Harvey. “A robot arm digital twin utilising reinforcement learning”. In: *Computers & Graphics* 95 (2021), pp. 106–114.
- [47] JR McGhee et al. “Strain sensing characteristics of 3D-printed conductive plastics”. In: *Electronics Letters* 54.9 (2018), pp. 570–572.
- [48] Nuwan Munasinghe et al. “3-D printed strain sensor for structural health monitoring”. In: *2019 IEEE International Conference on Cybernetics and Intelligent Systems (CIS) and IEEE Conference on Robotics, Automation and Mechatronics (RAM)*. IEEE. 2019, pp. 275–280.
- [49] Giovanni Postiglione et al. “Conductive 3D microstructures by direct 3D printing of polymer/carbon nanotube nanocomposites via liquid deposition modeling”. In: *Composites Part A: Applied Science and Manufacturing* 76 (2015), pp. 110–114.

- [50] Hauke Prüß and Thomas Vietor. “Design for fiber-reinforced additive manufacturing”. In: *Journal of Mechanical Design* 137.11 (2015).
- [51] Till Quadflieg, Oleg Stolyarov, and Thomas Gries. “Carbon rovings as strain sensors for structural health monitoring of engineering materials and structures”. In: *The Journal of Strain Analysis for Engineering Design* 51.7 (2016), pp. 482–492.
- [52] Devin J Roach et al. “The m4 3D printer: A multi-material multi-method additive manufacturing platform for future 3D printed structures”. In: *Additive Manufacturing* 29 (2019), p. 100819.
- [53] Seyed Hamid Reza Sanei et al. “Mechanical properties of 3D printed fiber reinforced thermoplastic”. In: *ASME 2019 International Mechanical Engineering Congress and Exposition, IMECE 2019*. American Society of Mechanical Engineers (ASME). 2019.
- [54] Patrick Scholle and Michael Sinapius. “A review on the usage of continuous carbon fibers for piezoresistive self strain sensing fiber reinforced plastics”. In: *Journal of Composites Science* 5.4 (2021), p. 96.
- [55] Aniruddha V Shembekar et al. “Trajectory planning for conformal 3d printing using non-planar layers”. In: *International Design Engineering Technical Conferences and Computers and Information in Engineering Conference*. Vol. 51722. American Society of Mechanical Engineers. 2018, V01AT02A026.
- [56] Baohui Shi et al. “Dynamic capillary-driven additive manufacturing of continuous carbon fiber composite”. In: *Matter* 2.6 (2020), pp. 1594–1604.
- [57] Martin Spoerk et al. “Anisotropic properties of oriented short carbon fibre filled polypropylene parts fabricated by extrusion-based additive manufacturing”. In: *Composites Part A: Applied Science and Manufacturing* 113 (2018), pp. 95–104.
- [58] *Technical Specifications*. Midwest Worldwide Import Company, LLC. 2022. URL: <https://www.captubes.com/specs.html>.
- [59] Xiaoyong Tian et al. “3D printing of continuous fiber reinforced composites with a robotic system for potential space applications”. In: *Proceeding of international symposium on artificial intelligence, robotics and automation in space*. 2016.
- [60] Shota Ushiba et al. “3D microfabrication of single-wall carbon nanotube/polymer composites by two-photon polymerization lithography”. In: *Carbon* 59 (2013), pp. 283–288.

- [61] Frank Van Der Klift et al. “3D printing of continuous carbon fibre reinforced thermo-plastic (CFRTP) tensile test specimens”. In: *Open Journal of Composite Materials* 6.01 (2016), p. 18.
- [62] Pawan Verma et al. “Synthesis and Characterization of Carbon Nanotube-Doped Thermoplastic Nanocomposites for the Additive Manufacturing of Self-Sensing Piezoresistive Materials”. In: *ACS Applied Materials & Interfaces* 14.6 (2022), pp. 8361–8372.
- [63] Zhenwei Wang et al. “Mechanical and self-monitoring behaviors of 3D printing smart continuous carbon fiber-thermoplastic lattice truss sandwich structure”. In: *Composites Part B: Engineering* 176 (2019), p. 107215.
- [64] Hans-Rudolf Weiss et al. “Workflow of CAD/CAM scoliosis brace adjustment in preparation using 3D printing”. In: *The Open Medical Informatics Journal* 11 (2017), p. 44.
- [65] CQ Yang et al. “Linear strain sensing performance of continuous high strength carbon fibre reinforced polymer composites”. In: *Composites Part B: Engineering* 102 (2016), pp. 86–93.
- [66] Xinhua Yao et al. “Evaluation of carbon fiber-embedded 3D printed structures for strengthening and structural-health monitoring”. In: *Materials & Design* 114 (2017), pp. 424–432.
- [67] Haiguang Zhang et al. “Hybrid Printing Method of Polymer and Continuous Fiber-Reinforced Thermoplastic Composites (CFRTPCs) for Pipes through Double-Nozzle Five-Axis Printer”. In: *Polymers* 14.4 (2022), p. 819.
- [68] Haoqi Zhang, Dongmin Yang, and Yong Sheng. “Performance-driven 3D printing of continuous curved carbon fibre reinforced polymer composites: A preliminary numerical study”. In: *Composites Part B: Engineering* 151 (2018), pp. 256–264.
- [69] Haoqi Zhang et al. “3D printing and epoxy-infusion treatment of curved continuous carbon fibre reinforced dual-polymer composites”. In: *Composites Part B: Engineering* (2022), p. 109687.
- [70] Da Zhao et al. “Fabrication and characterization of aerosol-jet printed strain sensors for multifunctional composite structures”. In: *Smart materials and structures* 21.11 (2012), p. 115008.
- [71] Peng Zhuo et al. “Material extrusion additive manufacturing of continuous fibre reinforced polymer matrix composites: A review and outlook”. In: *Composites Part B: Engineering* 224 (2021), p. 109143.

A Filament Test Piece

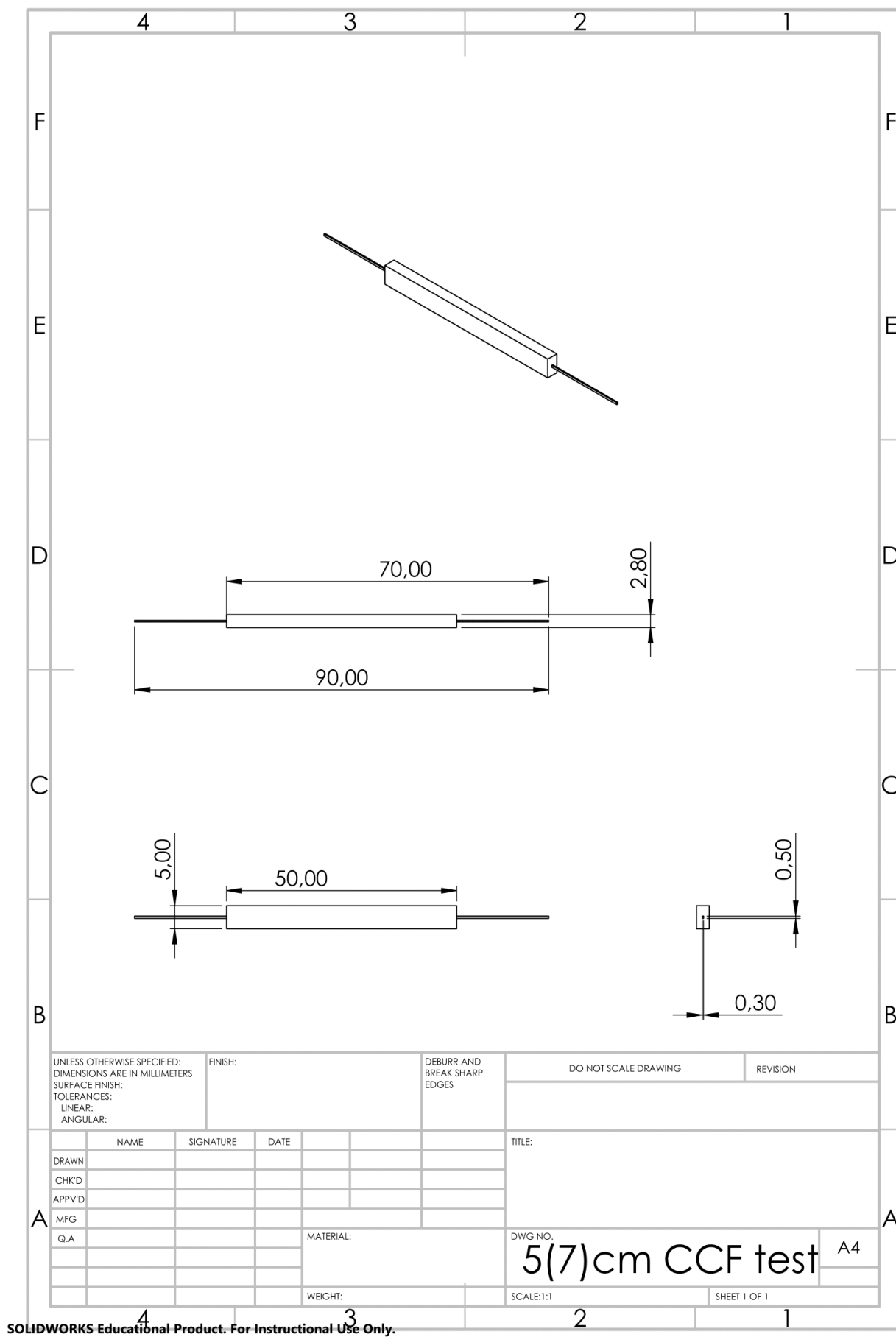


Figure 54: Filament test part for the manufacturability analysis.

B Backing Plate

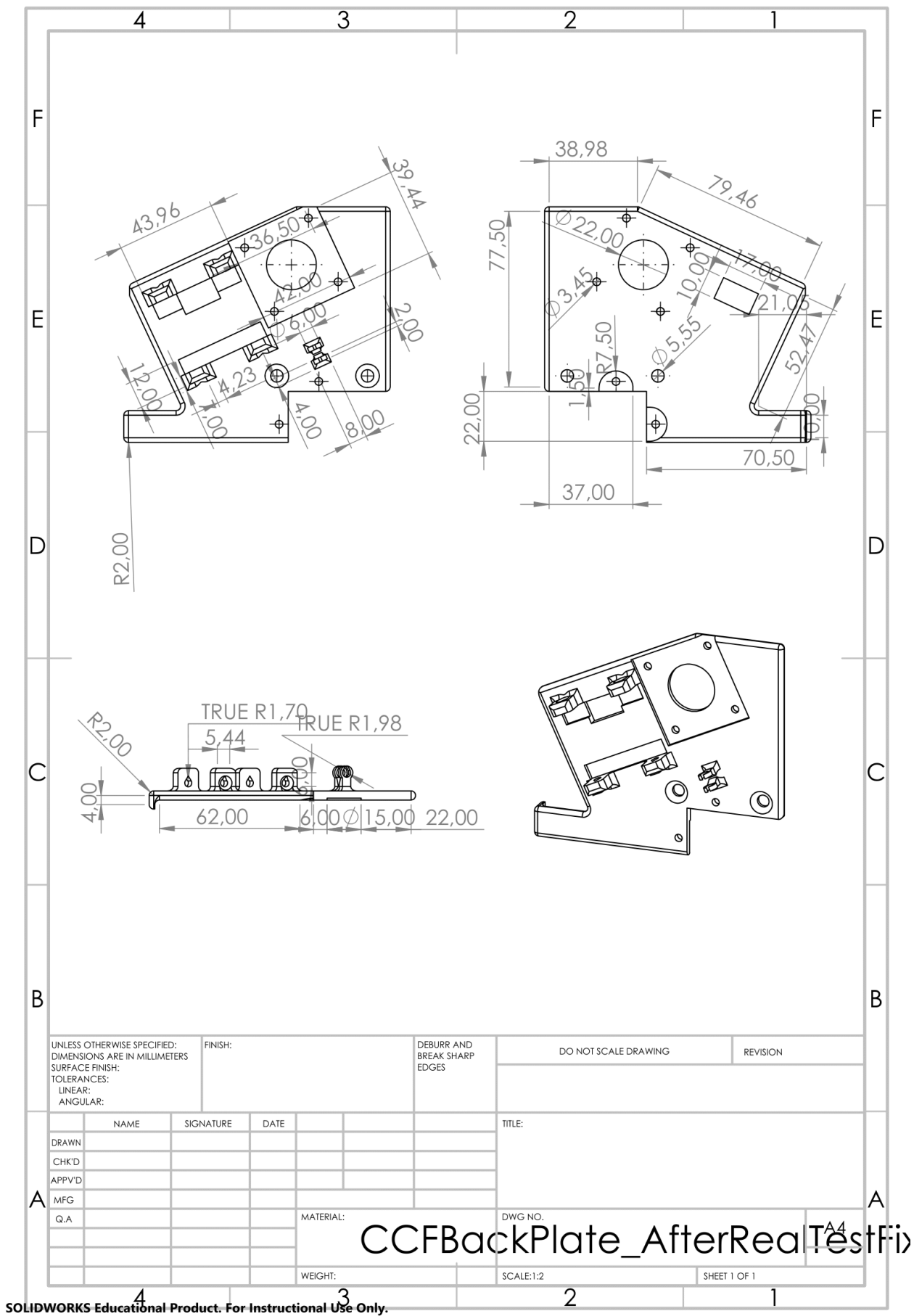


Figure 55: Backing plate housing the motors, cutting system and feeding system.

C Easy Print Fan Case

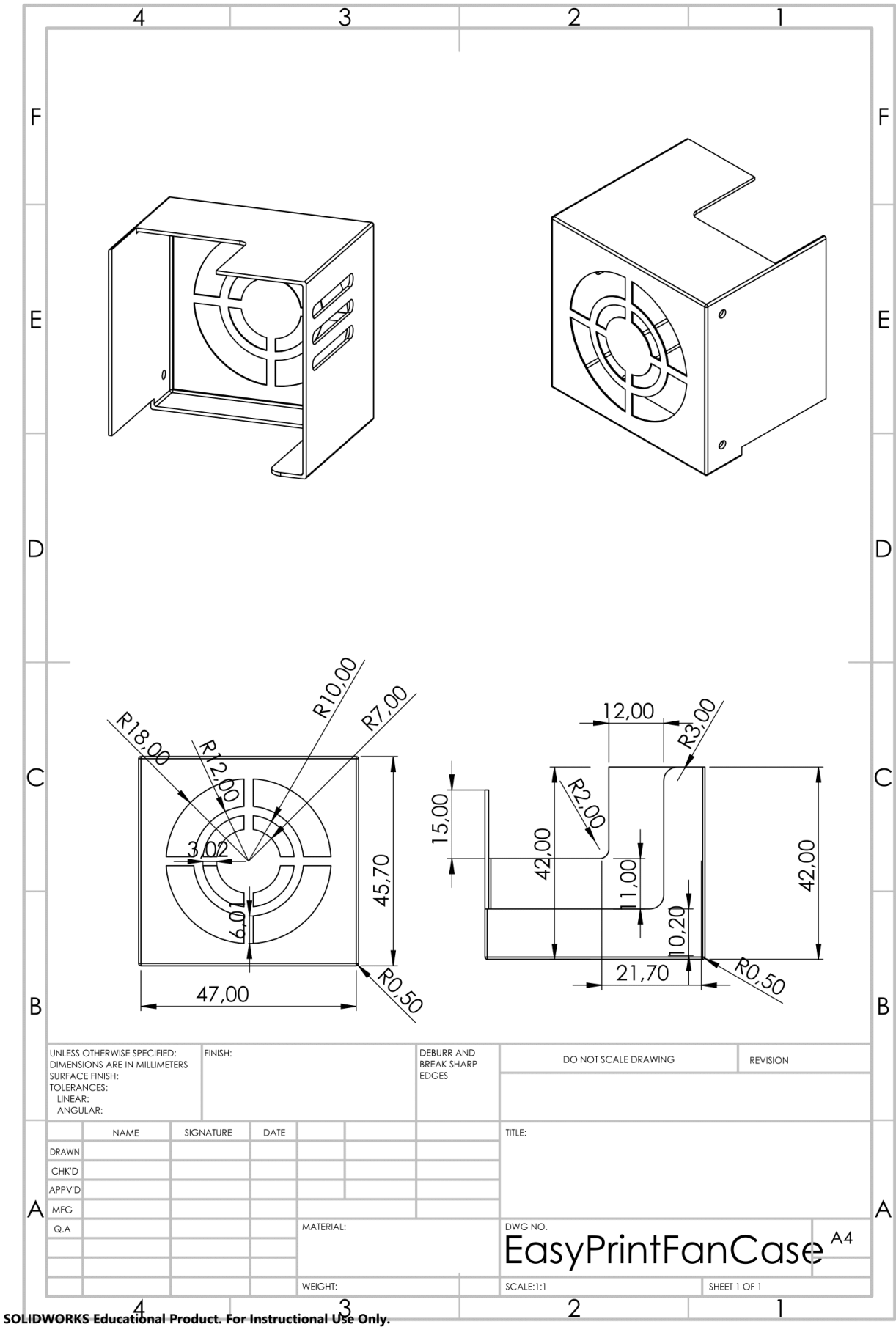
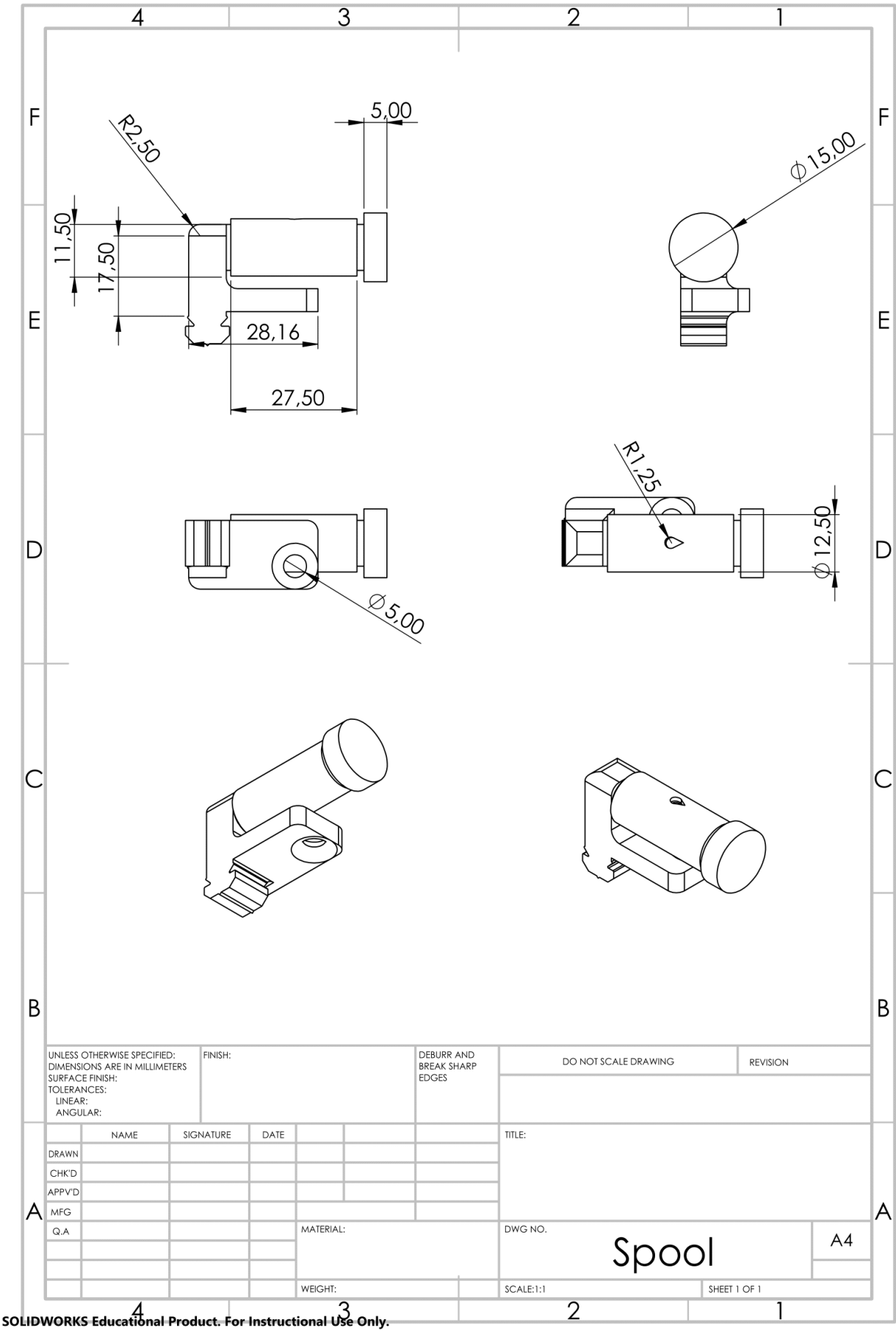


Figure 56: Fan case model altered to not require support material.

D Continuous Carbon Fibre Spool



E Fibre Cutting Arm

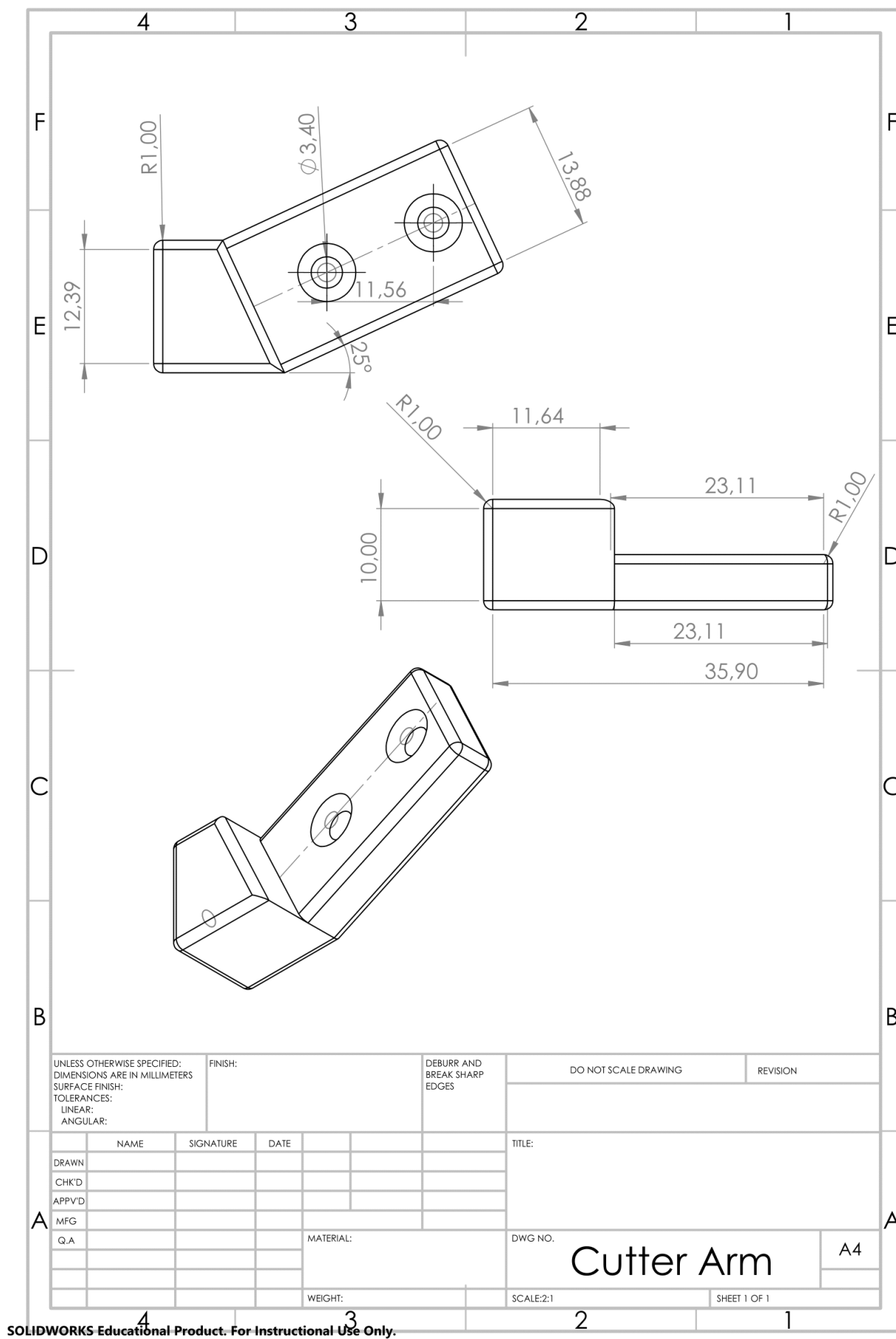
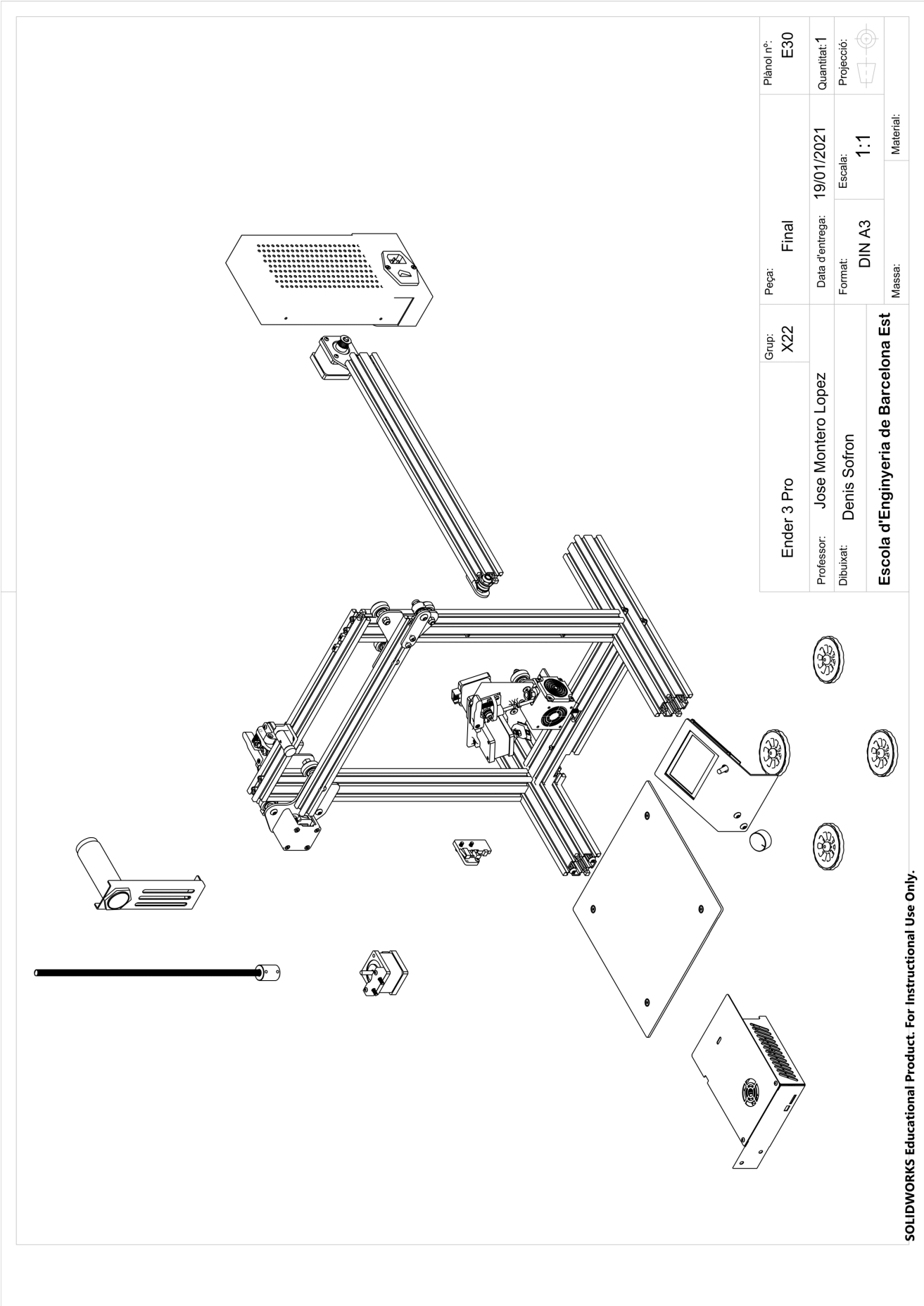


Figure 58: Cutter arm for cutting continuous carbon fibre.

F Continuous Pathing Cube



Figure 59: Cube for demonstrating continuous fibre placement.



SOLIDWORKS Educational Product. For Instructional Use Only.

Figure 60: Downloaded Ender 3 model.